Addis Ababa University

Addis Ababa Institute of Technology (AAiT)

School of Mechanical and Industrial Engineering

Fractural Analysis of S2 glass fiber/ SC15 Epoxy Reinforced composite Material using Numerical Method

A thesis submitted to the School of Graduate Studies of Addis Ababa University in partial fulfillment of the requirements of the Degree of Masters of Science in Mechanical Engineering (Mechanical Design)

By Bereket Teshome (GSR/5216/12)

Advisor: Dr. Mulugeta H. Mariam (PhD)

June 2024

Addis Ababa, Ethiopia

Addis Ababa Institute of Technology

School of Mechanical and Industrial Engineering

Approval of MSc. Thesis

Fractural Analysis of S2 glass fiber/ SC15 Epoxy Reinforced composite Material using Numerical Method

By Bereket Teshome

Approved by board of examiners

Dr. Mulugeta H. Woldemariam (PhD)	_____	_____
Advisor	Signature	Date
Dr. Araya Abera (PhD)	_____	_____
Internal Examiner	Signature	Date
Dr. Solomon Seid (Asso. Prof.)	_____	_____
External Examiner	Signature	Date
Dr. Araya Abera (PhD)	_____	_____
School Dean	Signature	Date
Dr. Sosina Mengistu (PhD)	_____	_____
Associate Director For PG program	Signature	Date

Declaration

This is to certify that this thesis is prepared by Bereket Teshome, entitled "Fractural Analysis of S2 glass fiber/ SC15 Epoxy Reinforced composite Material using Numerical Method" submitted in fulfillment of the requirement for the degree of masters of science in Mechanical engineering (Design stream).

Submitted By:

Bereket Teshome _____ _____

Student's Name Signature Date

Approved By:

Dr. Mulugeta H. Woldemariam (PhD) _____ _____

Advisor Signature Date

Acknowledgment

I want to start by giving thanks to God for his constant strength and support, even when it seemed impossible to write this paper. I would like to express my gratitude to Dr. Mulugeta H. Mariam, my advisor, for his constant support, direction, and advice throughout my studies. I also want to thank Addis Ababa University for creating excellent environment and for giving me the opportunity to study this programme. I want to express my gratitude to my parents, brothers, and my entire family for their unwavering love and support.

Abstract

Composite materials are utilized more extensively as a metal structure replacement in weight sensitive applications where energy and the environment are a real concern. This is due to their attractive properties as high strength-to-weight ratio and stiffness-to-weight ratio. Therefore, the replacement materials need to be studied and this research focused on numerical analyses of the interlaminar fracture behavior of S2-glass/SC15 epoxy composite. Glass fiber reinforced plastic (GFRP) composite structures are prone to fracture at interfaces or within the matrix which may not be visible from outside. Thus, a thorough knowledge of the initiation and propagation of cracks in GFRP composites is necessary.

In this study, fracture mechanics approaches used to analyze fracture parameters of Mode I and Mode II. A numerical method was used to model the S2-glass/SC15 epoxy composite as a plain weave lamina. According to ASTM standards, Double Cantilever Beam (DCB) and End-Notched Flexure (ENF) specimens were used for Mode I and Mode II interlaminar fracture behavior analysis, respectively. The Virtual Crack Closure Technique (VCCT), a finite element method was applied to study crack propagation using Abaqus software. The analysis was performed to study the loads at which the model begins to delaminate. The two models showed delamination within the range of the load application. The strain energy release rate along the delamination directions and across the crack fronts were also determined. The strain energy release rate value of the S2 glass / SC15 epoxy composite for mode I and mode II loading conditions were found to be 0.92 J/m² and 1.1 J/m² respectively. Through the determination of the strain energy release rate and analysis of load-displacement responses, significant findings were obtained. The study successfully characterized the delamination behavior of the composite laminate under both Mode I and Mode II loading, providing insights into its fracture mechanics properties. The investigation into the strain energy release rate offered a quantitative measure of the energy required for crack propagation, aiding in understanding the material's resistance to delamination.

Keywords: Interlaminar fracture, Virtual Crack Closure Technique (VCCT), BK law, DCB, ENF, strain energy release rate, ABAQUS

Table of Contents

List of figures

List of tables

Abbreviations

ASTM = American Standard Test Method

GFRP = Glass fiber reinforced plastic

LEFM = Linear elastic fracture mechanics

EEFM = Elasto-elastic fracture mechanic

FEM = Finite element method

DCB = Double cantilever beam

ENF = End notched flexure

ERR = Energy Release Rate

SERR = Strain energy release rate

CTOD = Crack tip opening displacement

DBT = time at bond failure

OPENBC = Opening behind crack tip at bond failure

CRSTS = Critical stress at bond failure

ENNRT = Effective strain energy release rate

VCCT = Virtual crack closure technique

CZM = Cohesive zone model

Nomenclatures

F =Force [N]

d = displacement [mm]

K = Stress intensity factor

G_{Ic} = Fracture toughness [J/m^2]

I = Moment of inertia [mm^4]

a_0 = Initial crack length [mm]

h = Height [mm]

b = Width [mm]

E = Young's modulus [MPa]

V_f = volume fraction of fiber

V_m = volume fraction of matrix

ρ_c = Density of composite [kg/m^3]

ρ_f = Density of fiber [kg/m^3]

ρ_m = Density of matrix [kg/m^3]

Chapter one

1. Introduction

1.1. Background of composite materials

Nowadays, the demand of composite materials in vehicle industry is highly increasing. The vehicle structure forms the backbone of a lightweight vehicles, it has a high capability of withstand the shock, vibration, twist, and stress and safely carry the maximum load for all design operating conditions. [1] In the automobile industry weight reduction is the important criterion. Fuel economy improvement and emission control are the two most important challenges the automotive industry faces today. Therefore lightweight materials, because of their greatest application in reducing fuel consumption and emission, are becoming a very popular material for vehicle structure alternative to conventional steel and cast irons, especially in automotive vehicles. Using materials like Aluminum and Steel increases the weight of the structure and this will decrease the efficiency of vehicles. So now a day lightweight composite materials like carbon fiber, glass fiber, epoxy glasses etc. are used as manufacturing material for vehicle structures. [2]

In addition to that in order to enhance specific properties of composites when exposed to fire, choice of inherently good resins and reinforcements is a very wide toolset in order for decrease flammability of the material and slow down the spread of the flame. [3] Thus Glass fiber reinforced plastic (GFRP) composites have been employed in vehicle industry because of their superior mechanical qualities, which make them desirable. The ability to resist fire and high strength-to-density value makes S2glass/SC15 epoxy composite very suitable for structural applications. [4]

Beyond that in vehicle production there must be reliable and proven fire resistant system. The application of flame retardants (FRs) reduces the overall fire risk associated with the use of highly flammable raw materials in goods such as textiles, garments, composites, plastics, etc., which plays a critical protective role in protecting life and property. Fire retardants are used

to slow the spread of fires or postpone the flashover period, giving people enough time to get away from the fire's potential dangers. [5]

Due to such mechanical properties of the composite, GFRP mostly considered in the vehicle production. However GFRPs show more failure modes when compared to metal materials. Composite materials that are mechanically loaded can have a variety of failures, including matrix cracking, debonding, delamination, and fiber breaking. Thus the fractural analysis of the composite material has to be studied in order to reduce the damage of the vehicle's component due to the different modes of failure. Among different types of failure mode of composite material, delamination (inter-laminar fracture) is the crucial one. This reduces the strength and stiffness of the structure of the composite and thus this minimizes the durability of the structure. [6]

In recent years, the failure of materials due to stress accumulation and crack initiation has been a major concern for designers after 1960 and it has been the main research area till now. Because of materials will start defect from its microstructure and leads to a massive destruction. [7]

Delamination (interlaminar fracture) is a prevalent issue with the interlaminar features of composites. It is caused by the separation of two adjacent lamina (plies). This failure mechanism is the main issue with laminated GFRPCs since it typically reduces the component's overall stiffness and load-bearing capacity, which ultimately causes the component to break as a whole and impairs its usefulness while it is in use. [8] [9] Therefore in this research the interlaminar fracture behaviour of S_2 glass fiber- SC15 epoxy determined under Mode I and Mode II loading conditions in order to overcome risks of failure in automotive applications.

1.2. Applications of composite materials in automotive industries

Composite materials are extensively used in various industries due to their unique properties and advantages. The automotive sector, which holds the highest market share for composites, is well-versed in using them. Composites not only allow for innovative car designs but also

contribute to lighter, more fuel-efficient vehicles. Automobiles need synchronised, dependable mechanisms made of parts resistant to fracture. Errors in the production or design will affect the product's performance and may cost the maker money. S2-Glass fiber/SC15 epoxy composite can be used in the automotive industry for lightweight structural components, such as body panels, chassis parts, and interior components. Its high strength-to-weight ratio and impact resistance make it an attractive choice for improving fuel efficiency and safety. The external body parts like door panels need to be very rigid and high resistant to fracture. [10]

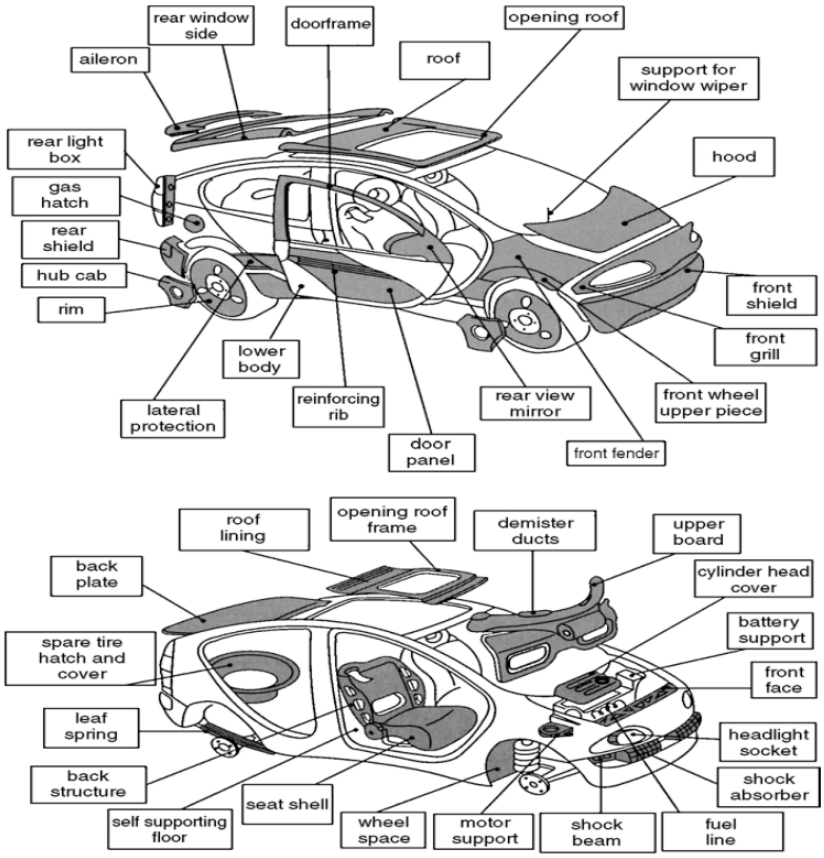

Figure 1.1 Composite materials application in automotive structure [10]

1.3. Fracture mechanics approach

Fracture mechanics is the field of solid mechanics that deals with the behavior of cracked bodies subjected to stress and strains. It was utilized to forecast and identify component of failure when a fracture already existed. The driving forces behind a crack are determined using

analytical solid mechanics techniques, while the resistance of the material to fracture is characterized using experimental solid mechanics techniques. In fracture mechanics, forces that cause fracture are classified in to three categories: these are direct load, chemical reaction and temperature. [7] This study focused only fracture due to the direct load application of the composite material.

The fracture mechanics theory made easiness and competence in designing a component respect to static and dynamic loading and assist in prevention of failures of structural and mechanical parts subjected to different loads in service. Theories behind the fracture mechanics, like LEFM and elastic fracture mechanic helped in analyzing the effect of loadings on the component, response of material under different loadings and fracture of material. [11]

In fracture mechanics, a stress intensity factor is calculated as a function of applied stress, crack size, and part shape. Failure happens when the stress intensity factor is higher than the material's fracture toughness.[12]

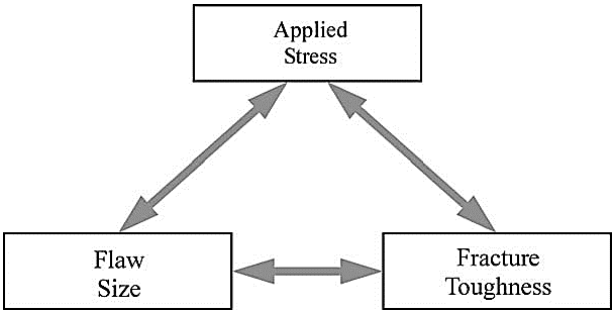

Figure 1.2 Fracture of mechanics approach. [12]

It is crucial to take fracture mechanics into account for a number of reasons. Cracks and defects resembling cracks appear far more frequently than one may anticipate. Cracks can occur spontaneously or as a result of severe stress or fatigue on a part. Fracture toughness usually decreases with increasing material strength.[8] Many engineers have an innate preference for materials with higher strengths, which might lead them in perilous directions. Failure of parts at loads lower than expected when employing a strength-of-materials approach might result from ignoring fracture mechanics. A brittle fracture failure happens quickly, catastrophically, and with little warning. [12]

1.3.1.1. Comparison between various types of fracture mechanics approaches

Fracture mechanics approaches encompass various methods and techniques used to analyze and predict the behavior of cracks and fractures in materials. A comparison of some commonly used fracture mechanics approaches are presented in table 1.1. The choice of the appropriate fracture mechanics approach depends on the specific problem, the level of complexity, the available computational resources, and the desired accuracy.

Table 1.1 Comparison between various types of fracture mechanics approaches. [13]

Approaches	***Description***	***Advantages***	***Disadvantages***
Virtual Crack Closure Technique (VCCT)	Calculates the energy release rate at the crack tip by relating the nodal forces and displacements near the crack tip.	- Computationally efficient - Can handle complex crack geometries	- Requires a priori knowledge of the crack path - Accuracy depends on mesh refinement near the crack tip
Cohesive Zone Modeling (CZM)	Models crack propagation by introducing cohesive elements or surfaces along the expected crack path.	- Can model complex crack paths without re-meshing - Captures the nonlinear fracture process zone	- Requires calibration of cohesive parameters - Computationally expensive for large-scale problems
Extended Finite Element Method (XFEM)	Extends the finite element method to model crack propagation without the need for re-meshing. The crack is represented as a discontinuity within the element.	- Can model arbitrary crack paths without re-meshing - Efficient for modeling crack initiation and propagation	- Requires special enrichment functions - Difficulty in imposing boundary conditions on the crack surface
J-Integral Method	Calculates the energy release rate at the crack tip using the path-independent J-integral.	- Provides a direct measure of the crack driving force - Applicable to elastic-plastic materials	- Requires accurate stress and strain fields near the crack tip - Cannot handle complex crack geometries and loading conditions

In this study, virtual crack closure technique (VCCT) is implemented due to its accuracy and compatibility with finite element method (FEM). ABAQUS provides built-in capabilities for implementing VCCT, making it readily available for users. Additionally, ABAQUS offers comprehensive documentation, tutorials, and user support, facilitating the implementation and utilization of VCCT for fracture analysis.

1.3.2. Linear elastic fracture mechanics

LEFM is a theory that deals with the crack analysis in linear elastic materials. It is based on the assumption that the stress field at the crack tip is elastic, and it provides a tool for solving most practical problems related to fracture mechanics.[14] The most important LEFM parameters are stress intensity factor (K), energy release rate and plastic zone. [15]

Energy release rate G, which is defined as the rate of change in potential energy with crack area for a linear elastic material. At the moment of fracture,$G = G_c$ the critical energy rate, which is the measure of fracture toughness. And for a crack length $2a$, the energy release rate is given by: [12]

$$G = \frac{\pi \sigma^2 a}{E}$$

Where, E is Young's modulus, σ is remotely applied stress and a is the half crack length.

1.3.3. Modes of fracture

The stress and material deformation in front of a crack tip depend on how the crack structure is loaded. In fracture mechanics the orientation of a crack with respect to the loading is defined by three main modes. Those are Mode I, Mode II and Mode III as shown in figure 1.3. [16] Mode I also known as opening mode is subjected to tensile stress that pulls the fracture faces apart. The sliding mode, or mode II, is characterized by a shear stress that slides the fracture faces parallel to the principal crack dimension. Shear stress is used in Mode III, or the tearing mode, to slide the crack faces perpendicular to the main crack dimension. [17]

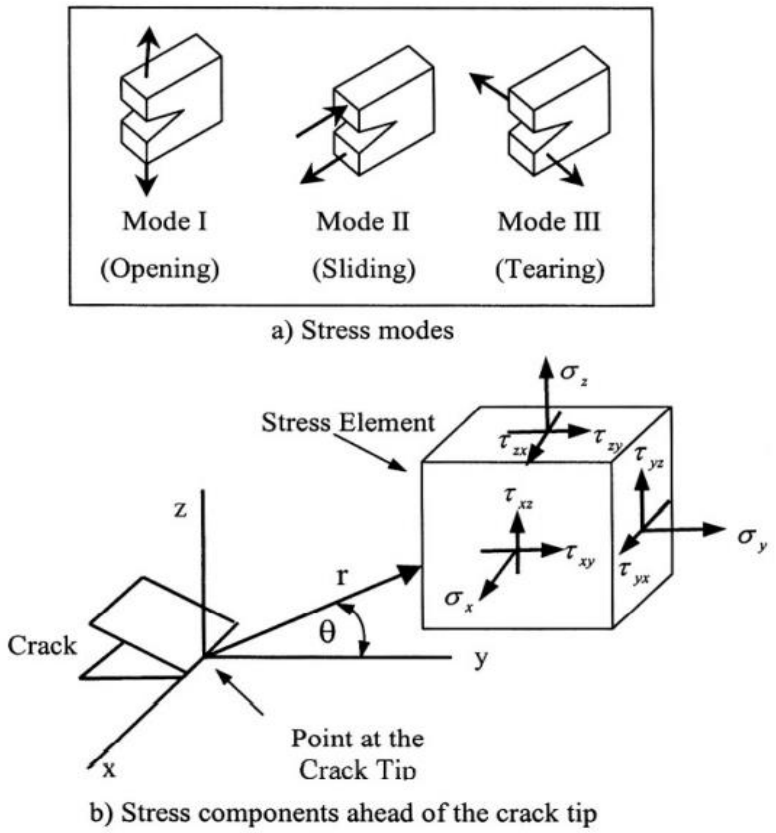

Figure 1.3 (a) basic loading modes for cracked body and (b) Crack coordinate system[18]

1.4. Statement of the problem

Laminated fiber reinforced plastic composites are particularly susceptible to failure by delamination as a result of a combination of compressive and bending stresses caused by the delaminated plies. Therefore it is crucial to understand the behavior of the fiber reinforced composites and also the various factors affect fracture behavior, particularly damage caused by delamination or interlaminar fracture.

These days, the vehicle production industry makes extensive use of composite materials like glass fiber reinforced plastic (GFRP) because of their fire retardant behaviour and lightweight qualities. However, they are very vulnerable to injury and lose a lot of their structural integrity due to the interlaminar crack. With the knowledge of the author, in previous works the delamination behaviour of S2glass/SC15 epoxy composite is not good enough. Thus, this research focused on the interlaminar fracture behaviour of S2glass/SC15 epoxy under mode I

and mode II loading condition using FEM in order to consideration in the designing of the material for the future.

Figure 1.4 A car with a crack on the door of GFRP composite material.[19]

1.5. Objective

1.5.1. General objective

The main objective of the study is to investigate the interlaminar fracture behavior of the S_2-glass fiber / SC15 epoxy-reinforced material for vehicle structure application using finite element method (FEM).

1.5.2. Specific Objective

- To identify the pattern of fracture parameters under mode I loading.
- To determine the strain energy release rate along the crack front under Mode I loading.
- To identify the pattern of fracture parameters under mode II loading.
- To determine the strain energy release rate along the crack front under Mode II loading.

1.6. Scope and limitation

The research concerns on the study of interlaminar fracture behavior of S2Glass/SC15 epoxy composites for vehicle application. Since it's costly to model the structure of the vehicle and undergo test, so the fracture analysis of the vehicle falls under using finite element analysis

software packages. DCB and ENF specimen as per ASTM standard are used in order to determine the strain energy release rate under mode I and mode II loading conditions respectively.

In addition to that, the reason behind that the research focused only on the numerical analysis was the complexity of the manufacturing process of the material. The difficulties was also in access of resources where the study is conducted. The use of the Virtual Crack Closure Technique (VCCT) in ABAQUS for delamination analysis allows for a non-destructive and cost-effective approach to investigate the behavior of composite structures. By validating the VCCT methodology through this research, it can serve as a benchmark for future simulations and provide confidence in the accuracy and reliability of virtual testing methods.

S2Glass/SC15 epoxy composites are commonly used automotive applications due to their high strength-to-weight ratio. By studying delamination in these specific composites, the research can have direct implications for the aerospace and automotive industries, where the prevention and mitigation of delamination are critical for maintaining structural integrity and performance.

1.7. Research methodology

In order to achieve the objective of this study various tasks are performed. A detail analysis was done on material characterization on the mechanical properties of S2Glass/SC15 epoxy composites, such as elastic modulus, Poisson's ratio, and fracture toughness. This was obtained from previous studies. The dimensions and layup of the composite specimen were determined by considering the required specimen size for the delamination tests.

A two-dimensional (2D) finite element model (FEM) of the composite specimen was modelled in ABAQUS. The delamination region was defined and a high-quality mesh established with appropriate meshing techniques to accurately capture the crack front.

Displacement -controlled boundary conditions were applied to simulate Mode I and Mode II loading conditions. The VCCT were implemented within the ABAQUS framework to calculate the energy release rate (G) and to perform the delamination simulations results,

including the delamination initiation and propagation behavior under Mode I and Mode II loading conditions.

1.8. Significance of the research

Studying the interlaminar fracture behaviour or delamination of S2 glass fiber/SC15 epoxy resin composite is significant for the vehicle industry due to several reasons. By studying delamination in S2 glass fiber/SC15 epoxy resin composites, researchers aim to improve the design, durability, and performance of composite materials used in the vehicle industry, ultimately leading to safer and more efficient vehicles.

The research will provide valuable insights into the delamination behavior of S2Glass/SC15 epoxy composites under Mode I and Mode II loading conditions. It will contribute to a better understanding of the mechanics and failure mechanisms associated with delamination in composite materials. By studying delamination in S2Glass/SC15 epoxy composites, the research can contribute to the development of improved design guidelines and analysis techniques for composite structures. This knowledge can be utilized to optimize composite manufacturing processes and enhance structural performance, leading to lighter, stronger, and more reliable composite components.

Understanding the delamination behavior of S2Glass/SC15 epoxy composites can aid in predicting the initiation and growth of delamination cracks. This knowledge is crucial for assessing the damage tolerance and structural integrity of composite materials, enabling engineers to make informed decisions regarding maintenance, repair, and replacement of composite components to ensure safety and reliability.

1.9. Organization of the thesis

This thesis is organized in to six chapters.

Chapter 1 discusses the background of the composite materials, the statement of the problem, the research objective, the scope and the significance of the research.

Chapter 2 present the studies or the literatures related to the interlaminar fracture behaviour of the glass fiber reinforced composite. Furthermore it discusses the classification of the composite materials and the interlaminar fracture behaviour of the composites.

Chapter 3 discusses the research methods, materials and procedures. It presented the research methodology, material selection and their properties briefly. In addition it identify the standard geometry of the specimen for the model. It also discusses the standards and the theoretical approaches or techniques used in FEA simulation as well as the unique attributes of the FEA package, i.e. ABAQUS.

Chapter 4 discusses the numerical analysis of the GFRP composite. It present briefly the models which are tested, the material properties and the plot which is resulted from the FEA.

Chapter 5 discuss the conclusions regarding with the research finding to restate the overall goal of the research and suggestions for further work.

Chapter two

2. Literature Review

This session reviews various literatures in depth to have a better understanding about the research status of composite materials, which leads to interlaminar fracture of composites which related to automotive application. It also covered a review on composite material, classification and the interlaminar fracture behaviour of composite.

2.1. Composite material

A composite material is created by macroscopically merging two or more components. The components do not dissolve in one another. One component is referred to as the reinforcing phase, and the matrix which it is embedded in it known for having a continuous nature. The material used in the reinforcing phase can take the shape of flakes, particles, or fibers. Composites are used because the overall properties of the composites are superior to individual components. [20]

2.1.1. Classification of composite material

There are two general classification systems of composite materials. The first is based on the matrix material (metal, ceramic, and polymer) and the second is based on the reinforcing material structure. [21]

2.1.2. Classification Based On Matrix Material

2.1.2.1. Metal matrix composite (MMC)

They consist of a matrix made of metal (copper, magnesium, aluminum, iron, cobalt) and a dispersed ceramic (carbides, oxides) or metallic (tungsten, lead, molybdenum) phase.

2.1.2.2. Ceramic Matrix Composites (CMC)

They consist of a ceramic matrix and embedded fibers of other ceramic material (dispersed phase).

2.1.2.3. Polymer matrix composite (PMC)

They consist of an unsaturated polyester thermoset matrix (UP), Epoxy (EP)) or thermoplastic (Polycarbonate (PC), Polyvinylchloride, Nylon, Polystyrene) and embedded, carbon, glass, steel or Kevlar fibers (dispersed phase).

2.1.3. Classification Based On Reinforcing Material Structure

The reinforcement material is one of the primary requirements in the strengthening mechanism of a composite, it is necessary to categorize the composites according to the characteristics of the reinforcement.

2.1.3.1. Particulate Composites

They consist a matrix reinforced by a dispersed phase in form of particles. Composites in which the particle orientation is random and composites where the particle orientation is favored. These materials' dispersed phase is made up of parallel-arranged, two-dimensional flat platelets, or flakes. [21]

2.1.3.2. Fibrous Composites

Short-fiber reinforced composites are made of a matrix reinforced by discontinuous fibers (length < 100*diameter) that are scattered throughout the matrix. They have divided into two orientation that are composites where the fiber orientation is random and composites where the fiber orientation is preferred. [21]

Long-fiber reinforced composites are made up of a matrix that is reinforced by continuous fibers that are scattered throughout the matrix. They have two orientations that are fiber orientation in a single direction and the fibers' bidirectional orientation (woven).[21]

2.1.3.3. Laminate Composites

A multilayer (angle-ply) composite is a fiber-reinforced composite made up of many layers with varying fiber orientations. [21]

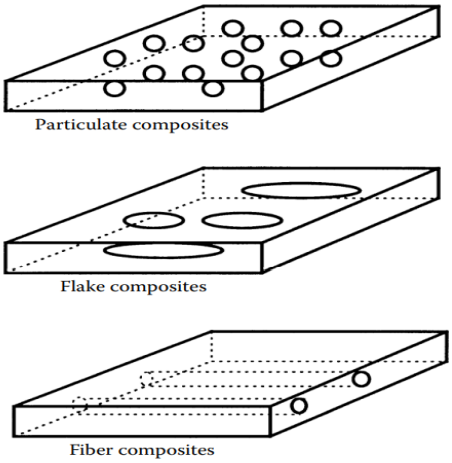

Figure 2.1 Geometrical representation of composite based on reinforcement shape. [20]

2.2. Interlaminar fracture behaviour of composite materials

Failure modes of composite materials are complicated and quite different from those of isotropic materials such as metals. The primary failure mechanisms that can occur are fiber matrix debonding, fiber fracture, matrix failure, and delamination. Among these failure modes, delamination due to interlaminar flaws is peculiar to composite laminates and may occur at ply drop-offs, edges, holes and around impact damage. The replacement of conventional materials by advanced composites is sometimes hindered due to their poor resistance to delamination growth. Therefore, the delamination problem must be understood before safer and more efficient composite structures can be designed. [11]

Standard specimens are used to analyze the failure modes in composites materials. Double cantilever beam specimen (DCB) used to determine the opening mode (MODE I) and end notched flexure (ENF) specimen used to determine the sliding mode (MODE II) interlaminar fracture behavior. [22]

Interlaminar fracture (delamination), it is mainly due to fiber bridging which is attributed to nesting (Figure 2.2). Johnson and Manalgiri stated that nesting is common in unidirectional layups where fibers migrate during the pressure/temperature cure cycle. Many investigations have observed fiber bridging along the crack opening sufficient to create a tied zone in various composites, such as carbon fiber composites, graphite fiber composites, glass fiber

composites, short glass fiber composites, woven graphite composites and woven Kevlar composites.[11]

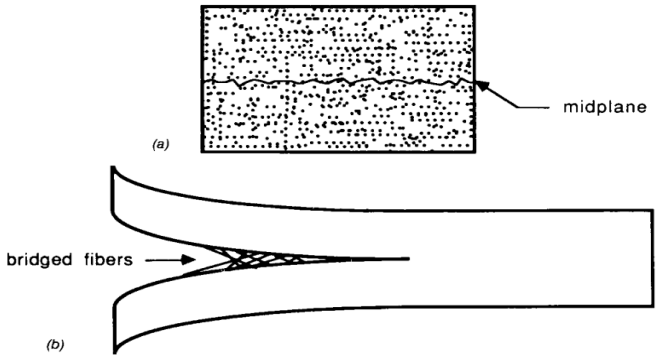

Figure 2.2 Schematic diagram of (a) nesting and (b) fiber bridging [11]

2.3. Fracture parameters

2.3.1. Stress intensity factor

In fracture mechanics, the stress condition close to the tip of a crack or notch generated by a remote load or residual stresses is predicted using a parameter called the stress intensity factor (K). It is a basic and helpful fracture mechanics parameter that characterizes the stress state at a crack tip, is connected to the rate at which cracks expand, and is employed to define fracture-related failure criteria. Based on applied stress, fracture size, and part geometry, the stress intensity factor is computed.

The strain energy release rate, or the stress intensity at the crack tip (K_C), gradually approaches a critical value. The stress intensity factor is used to compute the fracture stress of brittle materials. When the stress intensity factor exceeds the fracture toughness (K_{IC}) of the material, the crack propagates quickly and becomes unstable, ultimately leading to fracture.

The stress intensity factor (K) is given by;

$$K = Y\sigma\sqrt{\pi a}$$

Where, Y depends on the geometries of the crack, specimen and nature of loading. σ is the applied tensile stress, and a is the given crack dimension. [23]

2.3.2. Strain energy release rate

The strain energy release rate is a concept in fracture mechanics that measures the amount of energy released per unit area as a crack propagates through a material. It is an important parameter for understanding the behavior of cracks and predicting their growth and failure. When the crack grows straight forward, the strain energy release rate is directly correlated with the stress intensity component linked to a specific loading mode (Mode-I, Mode-II, or Mode-III). The strain energy release rate is also associated with the concept of crack growth. When a crack propagates through a material, the strain energy stored in the material is released.

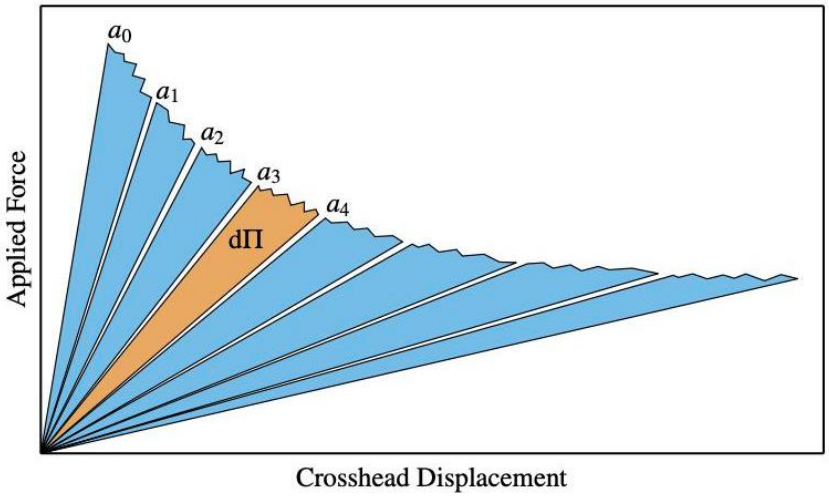

Figure 2.3 DCB test evaluation scheme in the associated force displacement curve. [24]

The strain energy release rate is given as: [22]

$$G = \frac{dU}{B\Delta a}$$

dU= total elastic energy in the specimen

B= specimen width

Δa= the change in crack length

2.3.3. Strain energy release rate relation to stress intensity factor

When the crack grows straight ahead, the energy release rate is directly correlated with the stress intensity component linked to a specific two-dimensional loading mode (Mode-I, Mode-II, or Mode-III). [25]

The strain energy release rate (G) for a crack under pure mode I or pure mode II loading in plane stress circumstances is correlated with the stress intensity factor by: [25]

$$G_I = K_I^2 \left(\frac{1}{E}\right)$$

$$G_{II} = K_{II}^2 \left(\frac{1}{E}\right)$$

Where the material assumed to be linearly elastic and according to the assumption, the crack extends in the same direction as the initial crack.

2.3.4. Crack tip opening displacement

Crack tip opening displacement (CTOD) is a measure of the distance between the opposite faces of a crack tip at the 90° intercept position. The point where two 45° lines cross the crack faces, beginning at the crack tip, is a commonly used, though arbitrary, location for measuring the distance behind the crack tip. The CTOD is a parameter used in fracture mechanics to measure the toughness of a material. [25]

The CTOD is defined as the displacement at the crack mouth, which is deduced by making the assumption that the specimen halves rotate around a stiff hinge. The CTOD is used to determine the critical crack size and the stress necessary for the crack to spread. The CTOD is also determine the fatigue life of a material.[26]

The CTOD is calculated using the following formula for plane stress condition: [26]

$$CTOD = \frac{P_{max}}{E}\sqrt{\frac{t}{w}}$$

Where P_{max} is the maximum load, E is the young's modulus, t is specimen thickness, and w is specimen width.

2.4. Standards used to design interlaminar fracture of composite materials

To show crack development and propagation regarding with interlaminar fracture, ASTM international provides their standard for DCB and ENF test.

DCB and ENF modelled as specimen following the standard dimensions and standard loading application as stated in ASTM to ensure accurate crack propagation and examine the fracture toughness.

DCB test method helps the determination of the opening Mode I interlaminar fracture toughness G_{Ic}, of continuous fiber-reinforced composite materials using the double cantilever beam (DCB) specimen. And ENF helps in determining the sliding mode interlaminar fracture toughness.

The specimen geometries with their corresponding modes of loading are represented in figure 2.4.

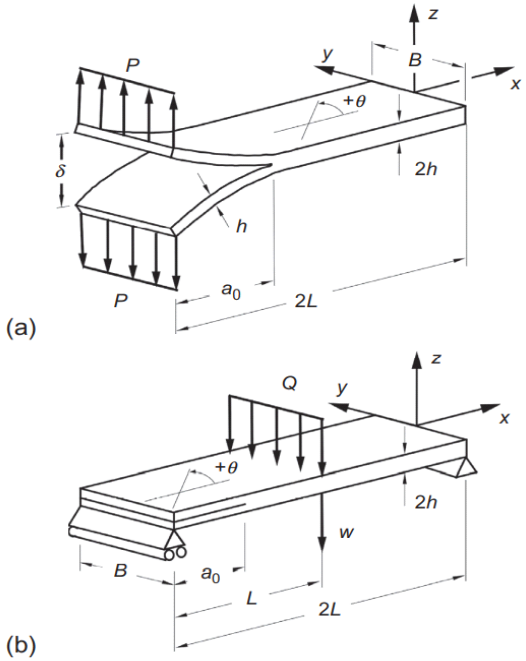

Figure 2.4 Standard test methods for delamination analysis (a) Double cantilever beam (DCB) specimen and (b) end-notched flexure (ENF) specimen [27]

Interlaminar critical strain energy release rates are calculated as follows:

Using the DCB test: [28]

$$G_{Ic} = \frac{96a_0^2P_{max}^2}{B^2h^3E_{11}}$$

Then the maximum displacement computed as:

$$d_{max} = \frac{2P_{max}a^3}{3EI}$$

$$I = \frac{Bh^3}{12}$$

Using the ENF test: [29]

$$G_{IIc} = \frac{9a_0^2P_{max}^2}{16B^2h^3E_{11}}$$

2.5. Literatures

R. Rikards [11], investigated the composite laminate's interlaminar fracture behavior under a variety of in-plane loading scenarios. With the help of the suggested compound version of the compact tension shear specimen, he was able to establish loading circumstances ranging from pure mode I through different mixed mode I/II ratios up to pure mode II. With the application of the modified virtual crack closure integral method and the finite element method, the mode I, mode II, and various combined mode I/II critical energy release rates at fracture start have been derived from the experimentally recorded critical loads. The parameters for a fracture criterion for the composite under this study have been established on the basis of the results.

K. Chawla et al. [22], investigated how reinforced short fibers affect the unidirectional laminate's interlaminar fracture toughness. The glass fiber laminates are made by hand lay-up process using a tidy and reinforced epoxy resin system. Interlaminar fracture toughness (G_{Ic}) of the laminates is measured using the double cantilever beam test and modified beam theory. In the case of short fiber reinforced specimens, the load vs. crosshead displacement plots exhibit consistent crack propagation in the tests with increased resistance to crack formation.

According to optical images, the use of fillers improves fiber bridging, increasing the laminate's G_{Ic} value in the reinforced casing by about 26%.

M.S. Sham Prasad et al. [30], in their study, they had discussed the experimental techniques used to assess the GFRP fracture toughness under different loading scenarios. They focused on the novel findings in experimental investigations of polymer matrix composites' intra- and interlaminar fracture toughness. They said that a thorough understanding of the material's reaction to the development of interlaminar fracture under the three modes and Mixed Modes is necessary to determine the life expectancy of composite structures. Thus, test procedures that are primarily based on the unique polymer matrix characteristics are provided and explored, making use of various fracture modes.

Robert et al. [31], they had done research on the interlaminar fracture characteristics of a graphite/epoxy composite material under opening, shearing and mixed mode conditions. Using a modified Arcan test fixture, they examined the interlaminar fracture properties for the ASI/3501-6 graphite/epoxy composite. They compared the experimental data with the key stress intensity factor, strain energy release rate, and quadratic interaction for mixed mode behaviour. They also came to the conclusion that there was a 9.1 factor of difference between the opening and shearing modes' essential fracture characteristics.

H. Jung et al. [32], they had conducted research on the fracture toughness of an epoxy interply hybrid composite reinforced with carbon fiber. They used a vacuum-assisted resin transfer moulding (VARTM) technique to conduct an experimental investigation of the inter-ply hybrid composites. They demonstrated that when the quantity of glass textiles increased, the interply hybrid composites' fracture toughness dropped. A linear equation can be used to represent how the glass fiber content increases with the decrease in fracture toughness. Test results demonstrated that the fiber arrangement has a major impact on the composite material's fracture toughness. Consequently, they concluded that when the glass fibers are distributed throughout multiple layers as opposed to a single layer, the glass fiber is efficient in enhancing the hybrid composite's fracture toughness.

A. Kojakin, et al. [33], their study was concentrated on the impact of surface treatment applied to glass fibers on the unidirectional laminates' interlaminar fracture toughness. Three distinct fiber surface treatments were taken into consideration: industrial fibers without further coupling agent treatments, saline treated fibers for strong bond strength, and polyethylene treated fibers for weak adhesion. Unidirectional glass fiber reinforced composites with varying fiber surface treatments have had their interlaminar fracture behaviour studied in mode I, mode II, and for a fixed mixed mode I/II ratio. For the purpose of determining the Mode I, Mode II, and mixed mode I/II critical energy release rates, they employed specimens with double cantilever beams (DCB), end notched flexures (ENF), and mixed modes (MMF). Analytical techniques were employed to examine the test data.

V. Prasada, et al. [34], they had presented a study that aims to investigate the impact of matrix modification on the flax fiber reinforced epoxy composites' interlaminar characteristics by the inclusion of Nano titanium dioxide (Nano TiO2) particles. Test specimens for double cantilever beams (DCB) and end-notched flexures (ENF) are utilized in Modes I and II to evaluate the interlaminar fracture toughness.. Using mechanical stirring and sonication, 50 nm-sized Nano TiO2 is mixed with the epoxy at loading rates of 0, 0.3, 0.4, and 0.5 weight percent. The process used for fabrication is compression moulding. The findings show that the inclusion of nanoparticles raises interlaminar fracture toughness values. The interlaminar fracture toughness values for Mode I and Mode II increased by 52% and 73%, respectively, for 0.4 and 0.5 weight percent TiO2. Infrared spectroscopy using Fourier transform is used to study structural characteristics. Images from scanning electron microscopy are used to assess failure mechanisms and the fiber matrix interface.

M. Herr´aez [35], he had studied the effect of the fiber cross section on the transverse strength of a unidirectional ply by means of computational micromechanics (CMM), making use of representative volume elements (RVE) under periodic boundary conditions (PBC). Fiber/matrix interface de-bonding is represented by means of a cohesive zone model (CZM) with a traction separation law, whereas a pressure dependent, Elasto-plastic model that includes tensile and compressive damage is employed to capture the nonlinear behavior of the

polymer matrix. The mechanical response of both constituents is calibrated using the properties obtained by the micromechanical tests.

S. N. A. Bt Safri et al. [36], they had conducted research on glass fiber reinforced composite damage assessments. They have talked about how the glass fiber-impacted specimens fail. Glass fiber type E-800 g/m^2 and type C-600 g/m^2 specimens with different thicknesses were subjected to low velocity impact tests and high velocity impact tests. The impact energy of the drop weight machine and the pressure of the single gas cannon were also changed. It was discovered that the specimens with the highest density and thickness sustained less damage area in high velocity impact tests. Tested at four different gas gun pressures, both types of glass fiber displayed damage in terms of fiber pullout and breaking. The laminates will go through matrix cracking and delamination processes prior to fiber failure. Compared to the type C-600 g/m^2, the type E-800 g/m^2 specimens showed less severe matrix damage. The experimental findings demonstrate that variations in thickness and mechanical characteristics have an impact on the damages sustained by the impacted glass fiber composites.

D. Rakshit et al. [37], they had concentrated on a combined experimental and numerical investigation in order to fully comprehend the fracture behaviour of fiber-reinforced plastic (FRP). To estimate the fracture parameters, such as fracture toughness and energy, ABAQUS is used in the finite element modelling of the FRP plate type of specimen. In accordance with American Society for Testing and Materials (ASTM) guidelines, three-point bending tests are another experimental method used to quantify the same parameters. A numerical model has also been developed using ABAQUS to simulate the same. They showed that the fracture toughness and fracture energy at mode I are found to be very close to each other, whereas they differ for mode II displacement.

2.6. Research gap

Designing and forecasting the structural integrity of different applications requires an understanding of the delamination behaviour of composite materials. To fully characterise the fracture behaviour of S2Glass/SC15 epoxy composites, it is necessary to investigate delamination under both Mode I and Mode II loading conditions.

The restricted study of the delamination behaviour of S2Glass/SC15 epoxy composites under Mode I and Mode II loading conditions represented as a research gap in this study. The requirement for a method to forecast the delamination resistance curve (R-curve) of S2Glass/SC15 epoxy composites under Mode I/II loading circumstances found to be another research gap. Moreover, there are no enough thorough research has been done to examine how S2Glass/SC15 epoxy composites delaminate under Mode I and Mode II loading scenarios.

Chapter Three

3. Research methods, materials and procedures

3.1. Introduction

The research methodology, material, and methods chapter is a crucial component of any research study. It serves as the backbone of the entire research process, providing a framework for the collection, analysis, and interpretation of data. This chapter focuses on the strategies and techniques employed to gather and analyze data, ensuring the validity and reliability of the research findings.

In this chapter, the fundamental principles and concepts that underpin the research methodology were discussed. By thoroughly understanding the research methodology, material, and methods employed in a study, readers gain insight into the credibility of the research findings. This chapter serves as a guide, providing transparency and clarity regarding the research process, ensuring the research study's integrity and contributing to the advancement of knowledge in the field.

This section details the specimens' selection for the analysis, including the selection of appropriate sample geometries and dimensions. It also outlines the material used and the delamination analysis and loading conditions.

3.2. Research Method

This study attained the basic research. In this paper, S2 glass / SC15 epoxy composite material for the vehicle structure is modelled and analyzed using ABAQUS Software. I took two samples of standard models that called end notched flexure (ENF) specimen and double cantilever beam specimen (DCB) in order to do the interlaminar fractural analysis.

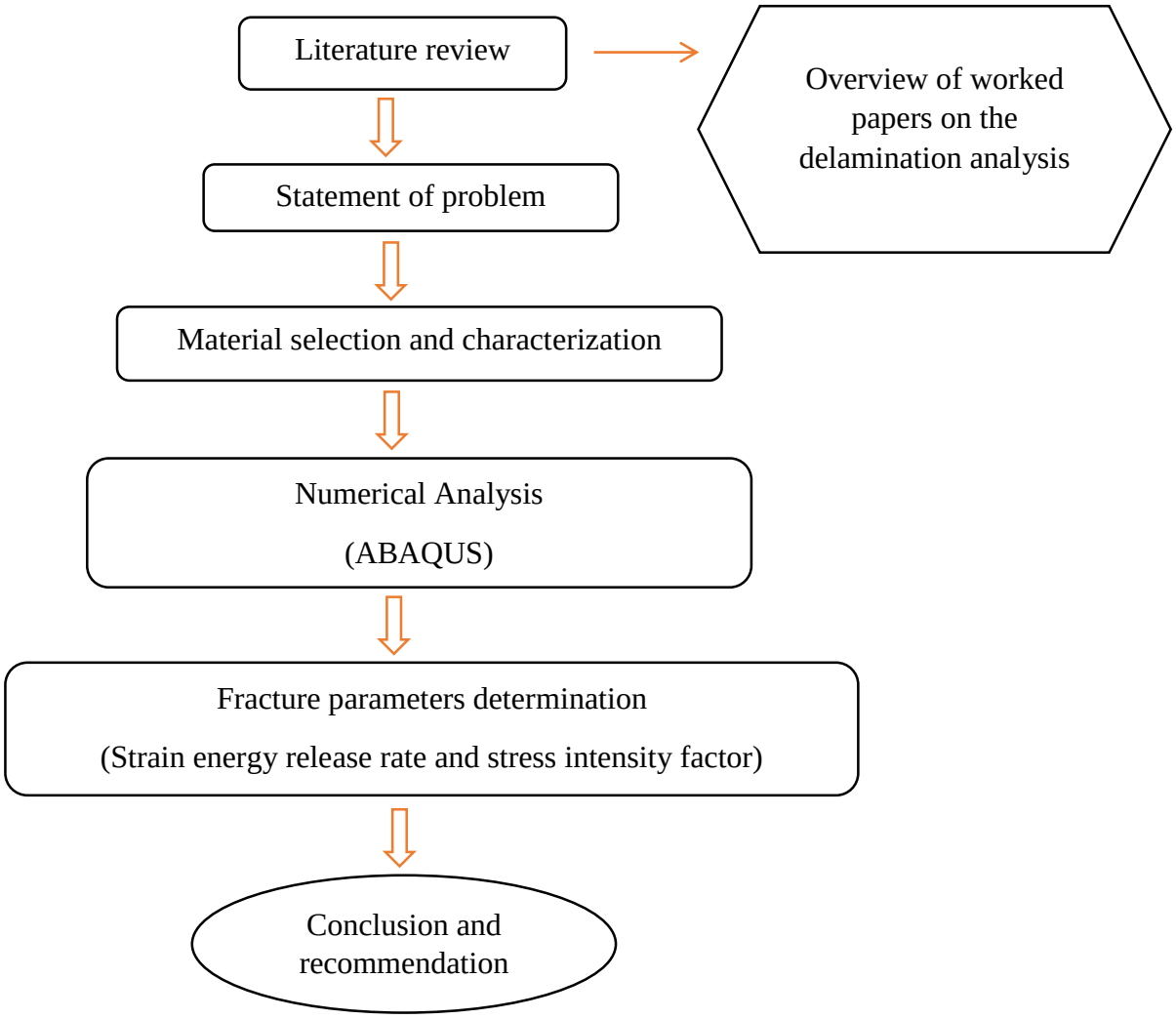

Figure 3.1 Research Methodology Diagram

3.3. Material selection and their properties

S2 glass / SC15 epoxy composite material is used in order to model double cantilever beam (DCB) and end notched-flexure (ENF) specimens to do the interlaminar fractural analysis.

S2-Glass fiber is selected because of its enhanced physical and mechanical properties such as light weight, high strength and stiffness. [38]

Minimizing the weight of the vehicle has a great impact in decreasing the fuel consumption. Because lightweight materials reduce the weight of power systems like batteries and electric

motors, they are particularly significant for enhancing the efficiency and range of hybrid electric, plug-in hybrid electric, and electric cars. [39]

Table 3.1 Mechanical properties of S_2 glass fiber.[40]

Fiber Type	*Density (kg/m^3)*	*Tensile Strength (MPa)*	*Young's Modulus (MPa)*	*Elongation (%)*	*Poisson's ratio*
S_2 glass	2460	4890	86900	5.7	0.22

SC15 epoxy matrix is selected because it act as a matrix element and widely used in industrial application because of their high strength and mechanical adhesiveness characteristic. It is also good solvent and have good chemical resistant at high temperature. [3]

The reason behind using SC15 Epoxy resin is its enhanced mechanical properties on fire retarding and excellent adhesion, good possibility of utilizing addition type reaction, its low shrinkage on curing, high fatigue resistance and superior flexural strength, and high chemical/corrosion resistance. [41]

Table 3.2 Material properties of SC15 resin material [42]

Resin Type	*Density (kg/m^3)*	*Viscosity @ 77^0F (cP)*	*Tensile Strength (MPa)*	*Young's Modulus (MPa)*	*Elongation (%)*
SC-15 Epoxy	1090	300	62	26200	6.0

Table 3.3 Material properties of S2glass/SC15 epoxy composite material [43]

Properties	*Symbol*	*Value*	*Unit*
Density	ρ	1.85E-06	kg/mm^3
Compressive strength	y	2910	N/mm^2
Tensile strength	T	58	N/mm^2
Young's modulus in the X direction	E_{11}	27100	N/mm^2
Young's modulus in the Y direction	E_{22}	27100	N/mm^2
Young's modulus in the Z direction	E_{33}	12000	N/mm^2
Poisson's ratio in the XY direction	v_1	0.11	-
Poisson's ratio in the YZ direction	v_2	0.18	-
Poisson's ratio in the XZ direction	v_3	0.18	-
Shear modulus in the XY direction	G_{12}	2900	N/mm^2
Shear modulus in the YZ direction	G_{13}	2900	N/mm^2
Shear modulus in the XZ direction	G_{23}	2140	N/mm^2
Layup	-	$[0,90,0,90]_S$	degree
Ply thickness	t	0.625	mm

Table 3.4 Material properties of steel for loading pins.

Properties	*Symbol*	*Value*	*Unit*
Young's modulus	E	133450	N/mm^2
Poisson's ratio	v	0.319	-

3.4. Stacking sequence and number of layers for S2/SC15 composite

The table below illustrates how different variety of S-glass is constructed, including the number of layers, orientation, and weave type. The pattern in which the fibers are woven together is known as the weave type. The quantity of S-glass sheets utilized to create the laminate equals the number of layers. The layer orientation is the direction in which fibers are aligned in each layer growth.

Table 3.5 Stacking sequence and number of layers for S_2 glass fiber/SC15 epoxy composite.[43]

Material	*Matrix*	*Fabric type*	*Layer construction*	*Target thickness (mm)*
S_2-Glass	SC-15	Plain weave $0^0/90^0$	8 Layers – $[0^0/90^0/0^0/90^0]_s$	6.35 - 7.62

3.5. ABAQUS CAE 2020

ABAQUS CAE 2020 is a powerful software tool that provides a user-friendly interface for creating, analyzing, and visualizing models in the ABAQUS simulation software. It simplifies the modeling process, supports customization and automation, and offers advanced meshing capabilities. [44] ABAQUS/CAE is designed to simplify the modeling process by providing a consistent interface. It allows users to create models, define material properties, generate meshes, submit and monitor jobs, and evaluate simulation results. [45]

Once the model is complete, ABAQUS/CAE generates an input file that can be submitted to the ABAQUS analysis product, such as ABAQUS/Standard or ABAQUS/Explicit. These analysis products perform the actual analysis based on the input file and generate an output database. The software also provides additional features and add-ons, such as CAD interfaces for importing and exporting CAD data, and the Composites Modeler for advanced modeling of composites. [46]

In order to accurately forecast the failure of composite structures, it is essential to describe the progression of delamination in laminates. This paper presents and evaluates an implementation of virtual crack closure technique (VCCT) utilizing a mode I and mode II formulation enabling for applicable BK- criterion while defining an effective debonding of lamina. The VCCT is offered by Abaqus/Standard for the modelling of progressive delamination progression. [47] In order to achieve this, a finite element models will be created with standard specimens and compared to the standard research findings from the literature, representing a laminate

specimen under pure mode I and pure mode II. Next, an assessment will be conducted to determine how the VCCT forms affect delamination progression and the specimen's load-displacement response.

3.6. Ply property analysis

GFRP composites are made up of multiple plies or layers of glass fiber reinforcement embedded in a polymer matrix. The properties of these individual plies, such as strength, stiffness, and failure behavior, are crucial in determining the overall performance of the GFRP composite structure. [48]

Table 3.6 Ply property analysis aspects. [48]

Aspects	***Description***
Material Characterization	- Determining the mechanical properties of the individual ply constituents - the glass fibers and the polymer matrix. - Measuring the fiber volume fraction, fiber orientation, and ply thickness.
Laminate Analysis	- Applying micromechanics models to predict the effective elastic properties of the individual plies based on the constituent properties. - Accounting for the orientation and stacking sequence of the plies in the laminate.
Failure Criteria	- Evaluating different failure theories, such as Maximum Stress, Maximum Strain, Tsai-Wu, Hashin, and Puck criteria, to predict the onset of failure in the individual plies. - Considering failure modes like fiber breakage, matrix cracking, and delamination.
Progressive Damage Analysis	- Modeling the gradual degradation of ply properties as the composite experiences increasing levels of loading. - Capturing the interaction between different failure modes and their impact on the overall laminate behavior.

3.7. Rule of mixture

The strength and modulus of fiber-reinforced composite materials are frequently predicted using "rule-of-mixture", which are on the basis of the matrix's weighted contributions and fiber filler. Considering the fiber's volume fraction V_f , matrix volume fraction V_m, and density of composites, ρ_c, can be computed using the subsequent formula: [49]

$$\rho_c = \rho_f V_f + \rho_m V_m \qquad (1)$$

Where for two components of composite the volume fraction is $V_f + V_m = 1$.

Similarly throughout the longitudinal direction, the unidirectional reinforced composites' elastic modulus, E_c is computed using: [49]

$$E_c = E_f V_f + E_m(1 - V_f) \qquad (2)$$

Where E_f and E_m are the elastic modulus of the fiber and matrix respectively.

Table 3.7 Volume fraction values of fiber and matrix material.

Material	*Density, ρ (kg/m^3)*	*Volume fraction, V*
S2 glass fiber	1090	0.49
SC15 epoxy matrix	2640	0.51

Table 3.8 Elastic modulus values of the S2 glass/ SC15 epoxy composite material.

Material	*Elastic modulus of fiber and matrix, E (MPa)*	*Elastic modulus of fiber and matrix, E_c (MPa)*
S2 glass/ SC15 epoxy composite	E_f = 27100	27100
	E_m = 27100	

3.8. Virtual crack closure technique (VCCT)

The Virtual Crack Closure Technique is a valuable tool for modeling interlaminar failure in composite materials and structures. The original purpose of the VCCT was to determine how quickly energy is released from a fractured body. Since then, it has been extensively employed in the laminate composites interfacial crack development simulation, presuming that the

interfaces serve as the constant channel for crack growth. The premise behind the VCCT is typically that a surface needs the equivalent quantity of energy to open as it does to close. The applied approach also makes the assumption that stress states surrounding the fracture tip remains unchanged. Considerably when the crack expands by a tiny amount (Δa). [50]

Energy release rates may be compute using VCCT, which depends on the results of solid (3D) and continuum (2D) finite element analyses.[27]

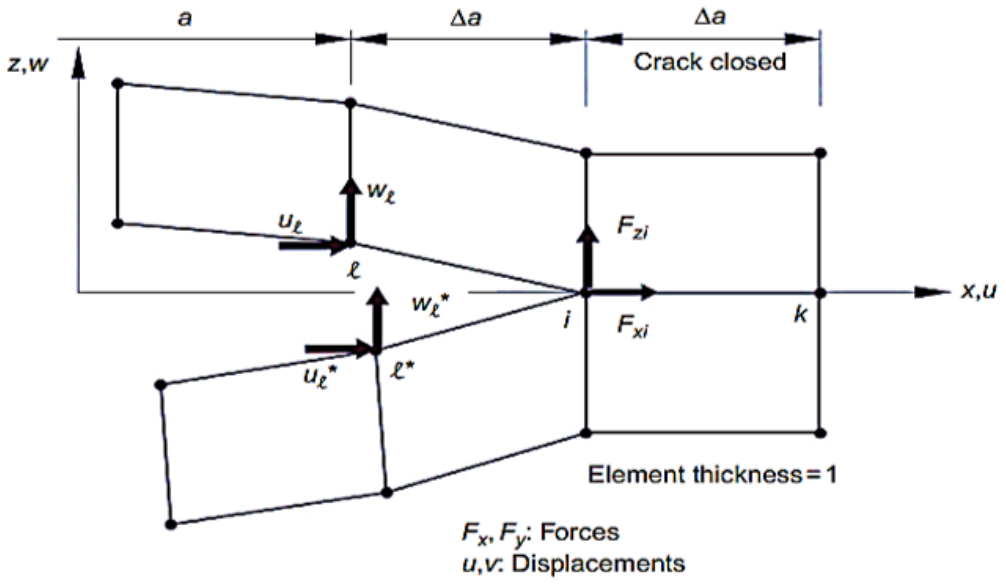

Figure 3.2. VCCT for 2D solid elements. [27]

3.8.1. Failure criteria

Failure criteria are mathematical models or guidelines used to predict the failure or fracture of materials under different loading conditions. The selection of an appropriate failure criterion depends on various factors, including the material properties, loading conditions, and the desired level of accuracy. [51]

Different failure criteria are presented in table 3.9.

Table 3.9. Comparison of different failure criteria. [51]

Failure criteria	***Description***	***Advantages***	***Disadvantages***
BK-Criterion	An energy-based criterion that considers the interaction between the Mode I (opening) and Mode II (shearing) fracture energies.	- Captures the mixed-mode fracture behavior. - Applicable to brittle materials	- Requires determination of fracture toughness parameters - May not be suitable for ductile materials
Maximum Strain Criterion	Predicts failure when any of the principal strains exceeds the corresponding ultimate strain of the material in that direction.	- Accounts for material anisotropy - Can be applied to nonlinear stress-strain behavior	- Requires accurate strain data - May not accurately capture failure modes
Tsai-Wu Failure Criterion	Uses a quadratic polynomial function of the stress components to predict failure. The coefficients are determined experimentally.	- Considers interaction between stress components - Can be applied to different failure modes	- Requires extensive experimental data to determine coefficients - Lacks physical interpretation
Hashin Failure Criteria	Predicts different failure modes (fiber tension, fiber compression, matrix tension, matrix compression) based on separate criteria.	- Captures different failure mechanisms - Provides better accuracy for composite laminates	- Requires more input parameters than simpler criteria - May be computationally intensive
Puck Failure Criterion	Predicts failure based on the fracture plane orientation and the stresses acting on that plane.	- Provides a fundamental approach to fracture - Applicable to brittle materials	- Requires knowledge of crack size and geometry - May not be suitable for ductile materials
Griffith's Criterion	Predicts failure based on the critical energy release rate required to propagate a pre-existing crack.	- Provides a fundamental approach to fracture - Applicable to brittle materials	- Requires knowledge of crack size and geometry - May not be suitable for ductile materials

3.9. BK Criterion

In this research, the energy-based Benzeggagh and Kenane (BK) failure criterion were implemented as represented by Equation (3). The BK (Benzeggagh-Kenane) criterion is commonly used in conjunction with the Virtual Crack Closure Technique (VCCT). The BK criterion is a popular choice for use along with the VCCT because it allows for the accurate prediction of mode I and mode II fracture in composites by considering the interactions between the different fracture modes. The combination of VCCT and the BK criterion provides a powerful tool for modeling crack propagation in composite structures. [47]

$$G_{equivC} = G_{IC} + (G_{IIC} - G_{IC}) \left(\frac{G_{Shear}}{G_T}\right)^{\eta} \qquad (3)$$

Where, η is the BK material parameter, $G_{Shear} = G_{II} - G_{III}$ and $\boldsymbol{G_T = G_{II} + G_{II} + G_{III}}$.

There are two ways to use the BK criterion in Abaqus. In the conventional BK option, the accumulated energy release rates G_{Shear} and G_T are used to compute the fracture toughness, G_{equivC}, which is provided in Equation 3.

3.10. Mesh convergence

Mesh convergence is the most crucial consideration in running most simulations. In order to get acceptable results mesh refinement should be analyzed in the model as the number of elements used in each mesh varied. As the mesh density raised, the numerical solution for the model will tend towards a unique value. According to various literature the mesh size for glass fiber composites is ranges from 0.1mm to 0.5 mm. [47], [52]

3.11. Development of the model

3.11.1. DCB specimen geometry and dimension

Double cantilever beam can be modeled as an elastic beam under point load. The beam has a rectangular cross-section and a specific material. [53]

According to standard test method for Mode I interlaminar fracture specimens shall be at least 125 mm (5.0 in.) long and nominally from 20 to 25 mm wide. [28]

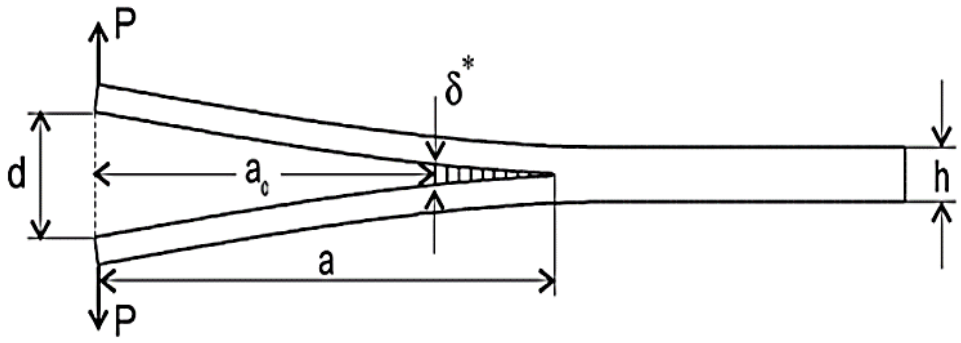

Figure 3.3 Geometry of double cantilever beam specimen. [54]

Assumption

1. Composite material S2-Glass fiber and SC15 epoxy matrix is used.
2. As it is a cantilever beam, the displacement at the one end is zero (the system is constrained at the one end). Opening forces are exerted to the DCB specimen by using loading blocks fixed to one end of the specimen.
3. All specimen dimension is taken based on standard model stated on the article of "Standard Test Method for Mode I Interlaminar Fracture Toughness of Unidirectional Fiber-Reinforced Polymer Matrix Composites", since the research is basically focused on the determination of the delamination.
4. The initial crack length is given to the model by considering the assumption of small results of *a/h* are not supported.

Table 3.10. Standard dimension for DCB specimen modelling on Abaqus.

Specimen	*Parameter*	*Dimension (mm)*
DCB	Length, *L*	150
	Width, *B*	20
	Height, *h*	5
	Initial delamination, a_o	55

3.11.2. Modeling of the DCB model on Abaqus using VCCT

The first stage was conducted, by modeling DCB using Abaqus. DCB test was used to estimate the Mode I interfacial fracture.

3.11.2.1. Part Model

The DCB has been modeled using the standard dimension from Table 3.10. The 2D DCB specimen is modeled as a solid part. The length of the DCB specimen is 150 mm and the width of 20 mm. It has two parts upper and lower composite.

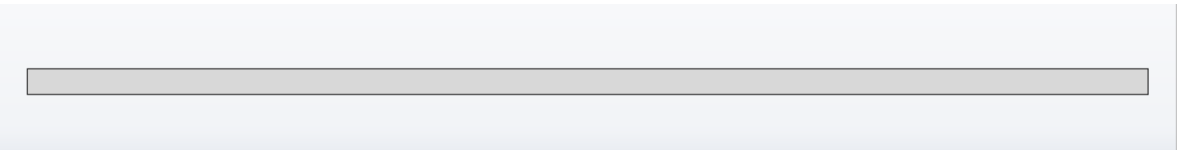

Figure 3.4 Part modelling of DCB on Abaqus.

3.11.2.2. Insert Material Properties

The material properties were assigned by inserting the material models stated in Table 3.3. A 4-node linear brick element was used, which considers the beam as a solid material. The composite materials were modeled as a solid material with a stacking sequence of lamina $[0/90/0/90]_s$ degree.

3.11.2.3. Creating and assigning section

A solid homogeneous section is assigned for the top and bottom parts.

3.11.2.4. Assembly of the model

The DCB specimen has two parts. The top and the bottom parts of the beam. These parts are assemble together in this step. In addition, a pre-crack length is defined between them by making partition on the upper surface of the bottom beam by using tools → partition → Edge → Enter parameter → Select the edge.

3.11.2.5. Creating Step and step increment

In this module the maximum number of increments had been specified in order to run the simulation. The minimum increment size must be small enough to ensure convergence of the simulation.

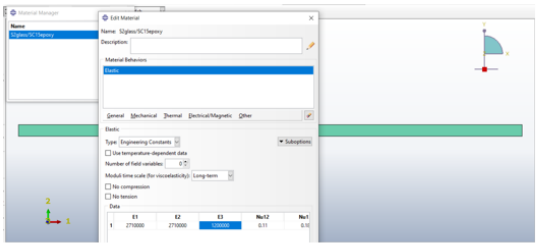

a) Input material property data for composite.

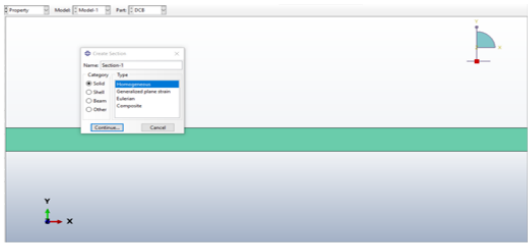

b) Creating section on Abaqus.

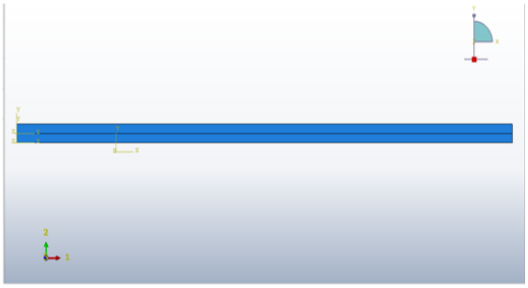

c) Assemble of top and bottom model DCB.

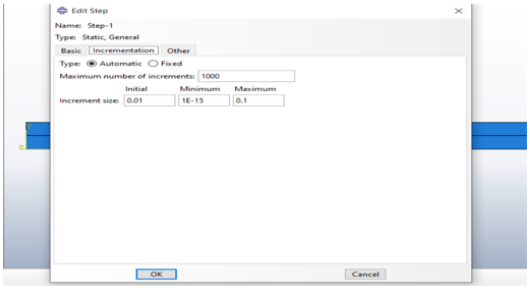

d) Creating step and step increment.

Figure 3.5 Assigning material property, sectioning, assembling and step increment on Abaqus for DCB modelling.

3.11.2.6. Field output request

Field output request is done for the model domain for every n increment, n=1 with output DBT (time at bond failure), OPENBC (opening behind crack tip at bond failure), CRSTS (critical stress at bond failure) and ENNRT (Effective strain energy release rate).

3.11.2.7. History output request

History output request done for DCB model at the left end of the DCB for every n increment, n=1, with output variable displacement U_2 and force F_2.

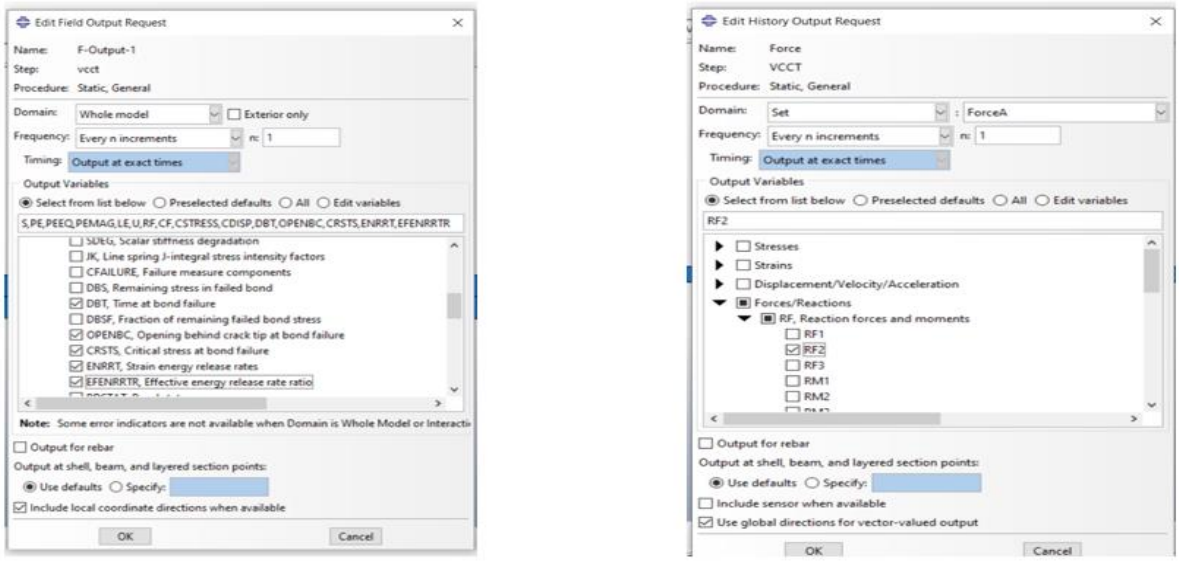

a) Field output request. *b) History output request.*

Figure 3.6 Field and history output request.

3.11.2.8. Creating Interaction and applying VCCT

In this module the interaction property will be specified for the model. This allows us to specify the behaviour of the contact interaction such as the type of sliding formulation, the discretization method and the contact tracking method.

The critical strain energy release rate values for mode I and mode II are presented in table 3.11 by using Young's modulus of the composite value.

Table 3.11 Interaction property of the DCB model using VCCT delamination approach.

Interaction Property	*Parameter*			
Fracture criterion	Critical strain energy release rate (KJ/m^2)			
	Mode I = 2.5525	Mode II = 1.6255	Mode III = 0	Exponent = 1.75

The interaction between the contacts created as node to surface and small sliding. And virtual crack closure used as the fracture criterion in order to simulate the delamination by limiting the bonded.

3.11.2.9. Meshing the model

The meshing was done by using quad structured element shape and a 4- node bilinear plane strain quadrilateral element type. The fine mesh were employed to precisely capture the failure of the material. The mesh refinement was done by applying different mesh sizes to the model. The recommended meshing sizes are taken from the literatures.

The study was carried out using three mesh sizes in order to develop fine mesh. The three mesh sizes were 0.3mm, 0.4mm and 0.5mm. These mesh sizes were selected based on literatures. [47], [52]

Table 3.12 Mesh size and their von miss stresses value.

Mesh size (mm)	*Maximum stresses (Pa)*
0.3	$52.99*10^2$
0.4	$45.35*10^2$
0.5	$49.74*10^2$

According to the comparison of the three DCB model the maximum percentage of change seen from mesh size 0.4 to 0.3mm mesh size. Thus, it showed that the effect of the mesh size.

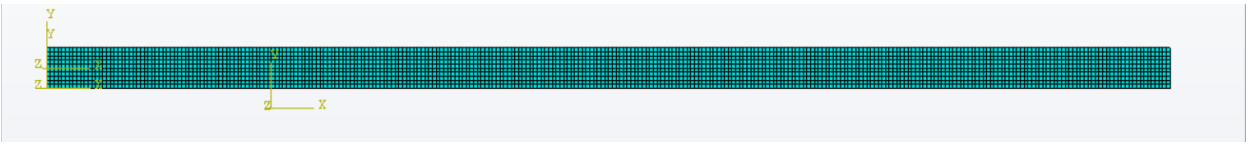

Figure 3.7 Crating mesh with 4-node bilinear plain strain quadrilateral element with approximate meshing size 0.5 mm.

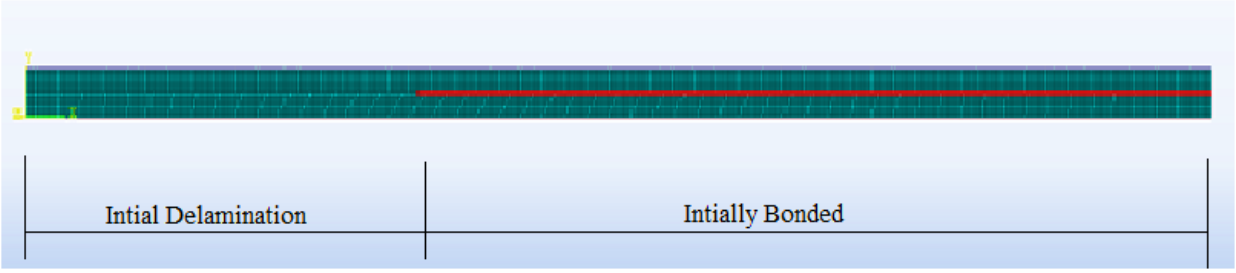

Figure 3.8. Initial delamination and bonded region of the DCB model.

3.11.2.10. Applying a boundary condition and a load to the model

The boundary condition and constraints for the DCB model are applied in this module of Abaqus. The right end of DCB is fixed and a magnitude of load 5 mm is applied on the upper and lower part of a beam in order to simulate the delamination by using load-displacement method. The DCB modelled with 4-node bilinear plain strain quadrilateral elements.

Table 3.13. Boundary condition applied to the DCB model.

Reference Point	U_1	U_2
1(Top)	0	5 mm
2(Bottom)	0	-5 mm

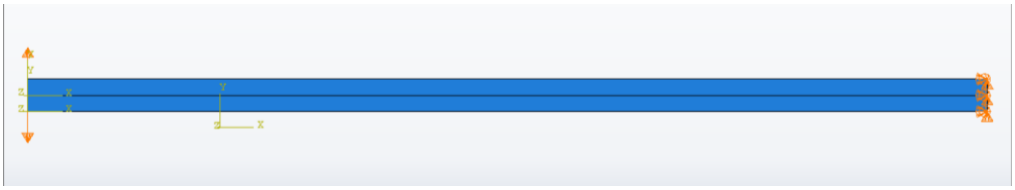

Figure 3.9. Boundary condition and loading to the DCB model.

3.11.3. ENF specimen geometry and dimension

Mode II interlaminar fracture delamination test could be analyzed using ENF specimen with span length of 100mm and pre-crack insert 30mm. And a loading pin at the center and two supporting pin at both ends are used. [29]

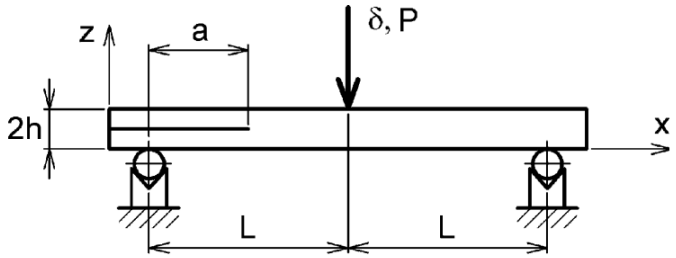

Figure 3.10. ENF Specimen geometry. [29]

Table 3.14. Geometry for ENF specimen modelling on Abaqus.

Specimen	*Parameter*	*Dimension (mm)*
ENF	Length, *2L*	100
	Width, *B*	20
	Height, *2h*	6
	Initial delamination, a_o	30
	Loading pin diameter, D_1	20
	Support pin diameter, D_2	10

3.11.4. Modelling of ENF on Abaqus using VCCT

3.11.4.1. Part modelling of ENF specimen

The ENF specimen has two parts: the lower and the bottom. It is modelled as shell planer using the standard dimension according to ASTM international. It uses a rectangular cross section element with three roller support.

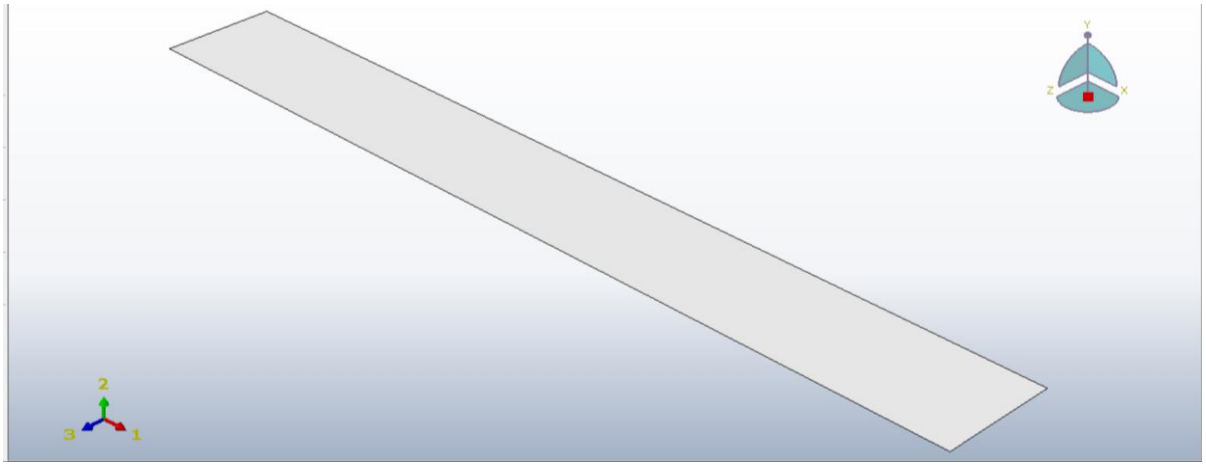

Figure 3.11. Part model of ENF specimen.

3.11.4.2. Defining material properties

In this module the composite S2glass/SC15 epoxy material is used and its material properties defined.

3.11.4.3. Assigning Section

A composite section assigned to an ENF specimen with continuum shell. The ENF modelled as composite material with eight layers with stacking sequence of $[0/90/0/90]_s$.

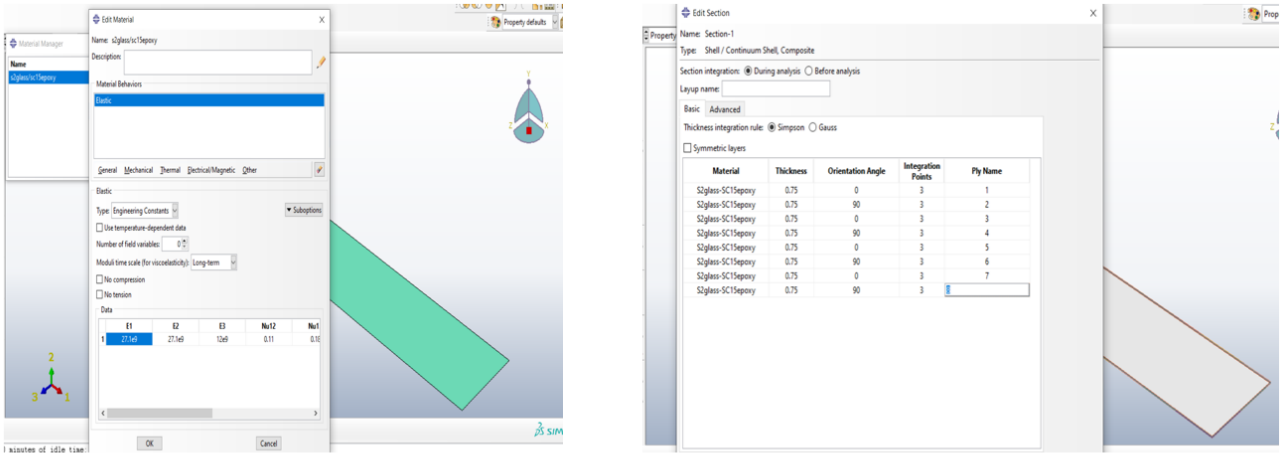

a) Defining material properties of S2glass/SC15 composite. *b) Creating section for the composite with* $[0/90/0/90]_8$

Figure 3.12. Assigning material property and sectioning on Abaqus for ENF modelling.

3.11.4.4. Assembly of the ENF model

The ENF specimen is located on a three-point bending fixture with the loading points positioned at equal distances from the notch.

The three-point bending fixture consists of two support rollers and a loading roller. The support rollers are placed at equal distances from the loading roller. The ENF is located on the support rollers with the notch centered under the loading roller. An initial crack length of 30mm is inserted.

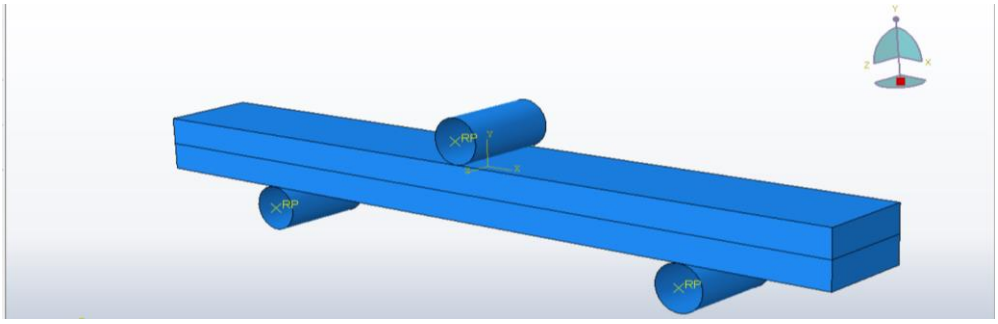

Figure 3.13. Assembly of the ENF model.

3.11.4.5. Creating Step and Step increment

In the Increment size field, specify the initial increment size. The initial increment size should be small enough to ensure convergence of the simulation.

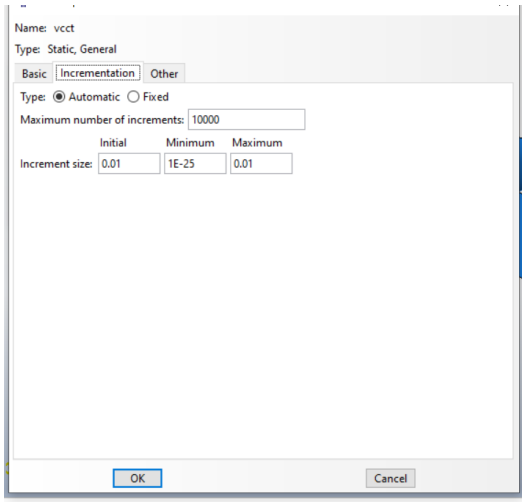

Figure 3.14. Creating step on Abaqus.

3.11.4.6. Creating interaction on Abaqus

In this step I had specify contact interaction behaviour, such as the type of sliding formulation, the discretization method, and the contact tracking method. The interaction between the contacts created as node to surface and small sliding. And virtual crack closure used as the fracture criterion in order to simulate the delamination by limiting the bonded.

3.11.4.7. Applying boundary condition and load

In this part the boundary condition applied at the nodes, and the degrees of freedom be constrained, and magnitude of the load applied is 10mm.

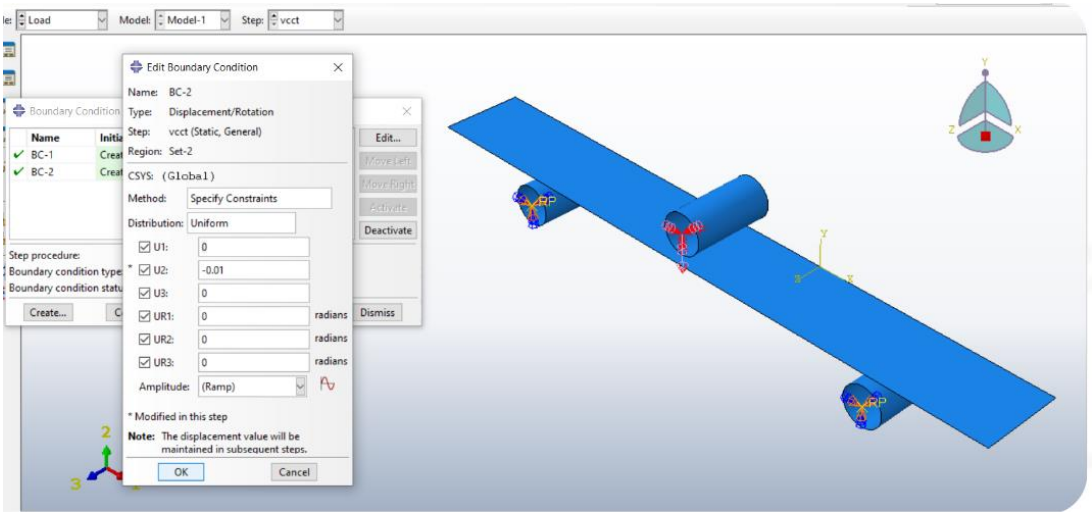

Figure 3.15. Application of all boundary conditions and load.

3.11.4.8. Defining mesh

The fine mesh around the notch employed to precisely capture the material fracture behaviour near the notch. The ENF model meshing is done by using quadrilateral structured a 4-node doubly curved shell element. And the meshing approximate global size is 0.002 mm.

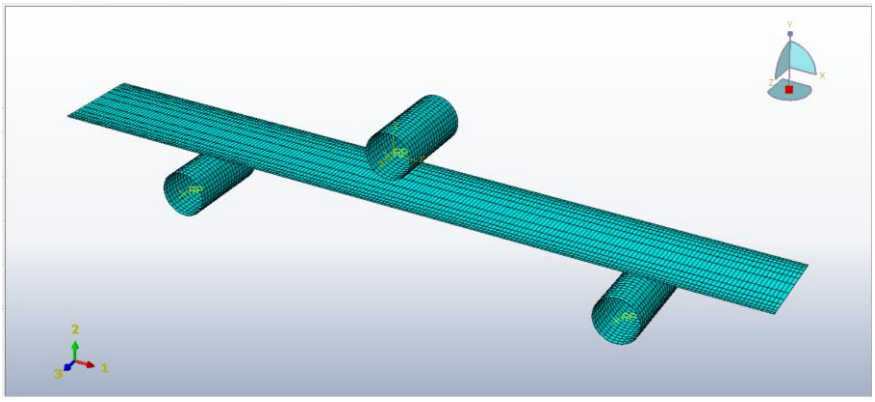

Figure 3.16. ENF model with approximate meshing size 0.002 mm.

Figure 3.17. Initial delamination and bonded region of the ENF

3.11.4.9. Creating special crack debonding using VCCT

A crack is crated using “Special” from tab menu in order to simulate VCCT debonding.

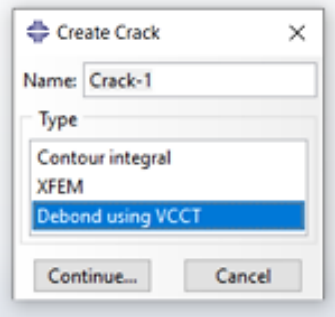

Figure 3.18. Creating special crack debonding using VCCT.

Chapter Four

4. Results and Discussion

4.1. Introduction

The delamination analysis of S2glass fiber/SC15 epoxy composite presents a comprehensive investigation into the delamination behavior and failure mechanisms of this specific composite material. Delamination, which refers to the separation or detachment of layers within a composite material, is a critical concern in structural applications as it can significantly compromise the material's integrity and performance.

The objective of this research study is to gain a deeper understanding of the factors influencing delamination in S2glass fiber/SC15 epoxy composite and to propose strategies for mitigating delamination-related issues. By examining the interfacial properties, mechanical behavior, and failure mechanisms of the composite material, this study aimed to contribute valuable insights to the field of composite materials and assist in the development of more robust and reliable structures.

This chapter discussed the simulation results obtained from the delamination analysis. This includes the characterization of the delamination behavior, including the critical stress levels or energy release rates at which delamination initiation and propagation occur. And key findings such as load-displacement responses and strain energy release rate of the material are briefly discussed for interpreting the delamination behaviour of the S2glass fiber/SC15 epoxy composite and drawing meaningful conclusions.

4.2. Results of DCB delamination using VCCT

Figure 4.1 (a) and (b) displays the DCB specimen's with deformed shape. Under the applied load, the specimen has deformed, and crack propagation has occurred. It also shows the von Mises stresses which are greatest close to the crack tip. This occurs as a result of the high concentration of stress near the crack tip. The specimen may fail due to the forces near the

crack's tip spreading the crack. Thus, by using this information, the specimen can be designed to avoid failure or new materials that are more resilient to failure can be created.

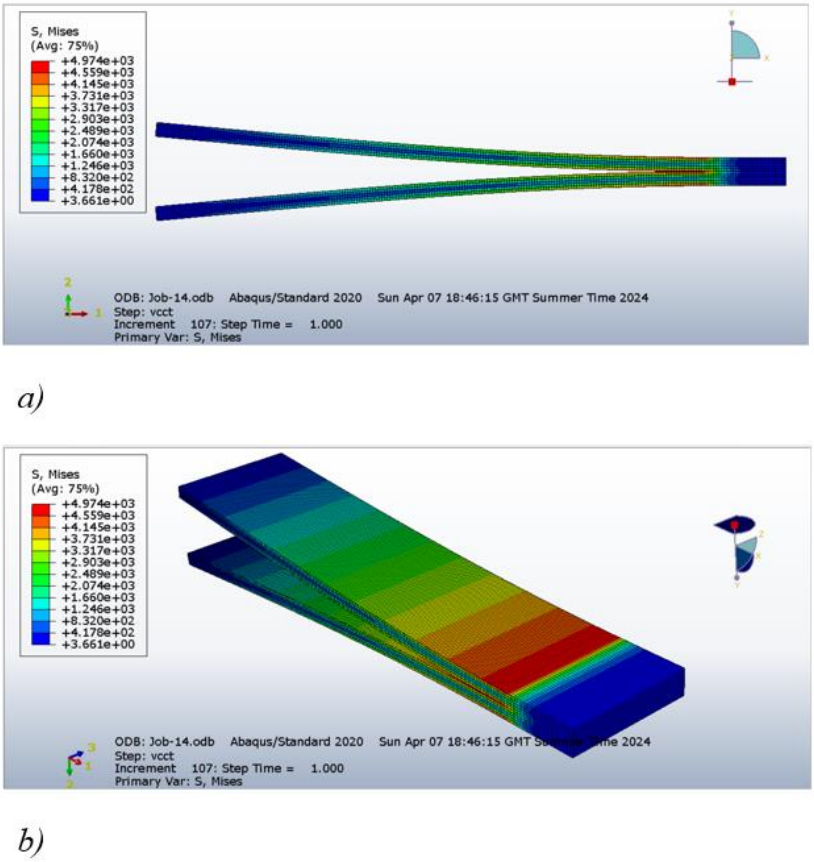

Figure 4.1. The stress propagation along the crack path in Pa (a) and along the crack front position (b).

The delamination began when the magnitude of the load equals to 84.1635 N and the opening displacement 1.833 mm.

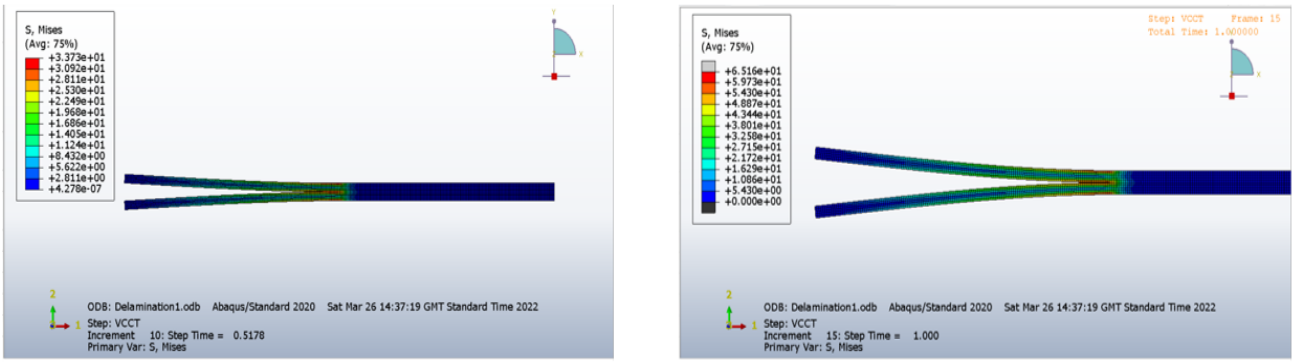

a) *b)*

Figure 4.2. DCB simulation under mode I loading showing with two step time increment starting with initial delamination of 55mm.

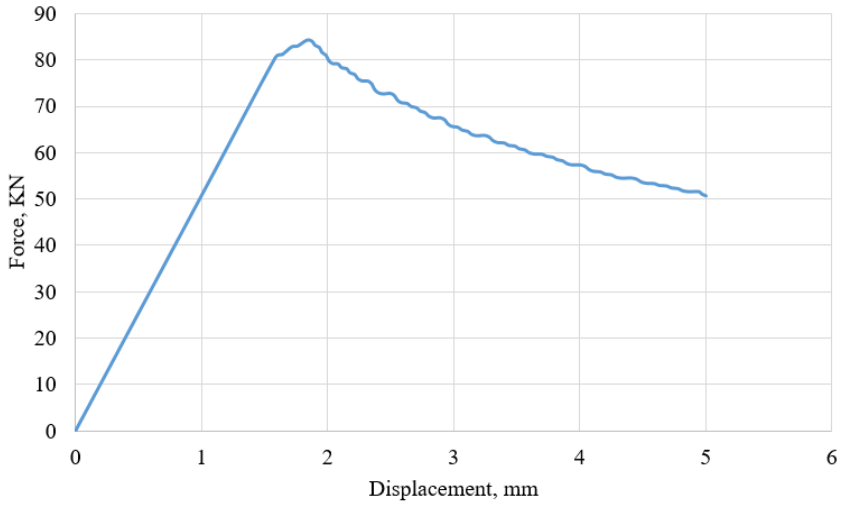

Figure 4.3. Force-displacement graph of the DCB model

Figure 4.3 shows the force-displacement curve of DCB simulation performed in Abaqus. The curve is divided into two distinct regions: The linear region shows the force required to displace the beam increases linearly with displacement. This is because the beam is behaving elastically, meaning that it retain its original shape after the removal of force. Then the nonlinear region shows the force required to displace the beam increases at a slower rate. This is because the crack is propagating, and the beam is becoming less stiff.The curve shows that as the load is applied, the crack begins to open, and strain energy increases. The slope of the

curve at this point reflects the material's stiffness and resistance to crack initiation. Once the crack starts propagating, the strain energy may reach a plateau or increase steadily. This phase indicates a balance between the energy required for crack growth and the energy released as the crack extends. Generally, the shape of the curve reveals how the strain energy changes as the crack propagates under mode I loading.

A material with a higher strain energy release rate will exhibit a higher resistance to crack propagation, which will be reflected in a steeper curve in the force-displacement plot.

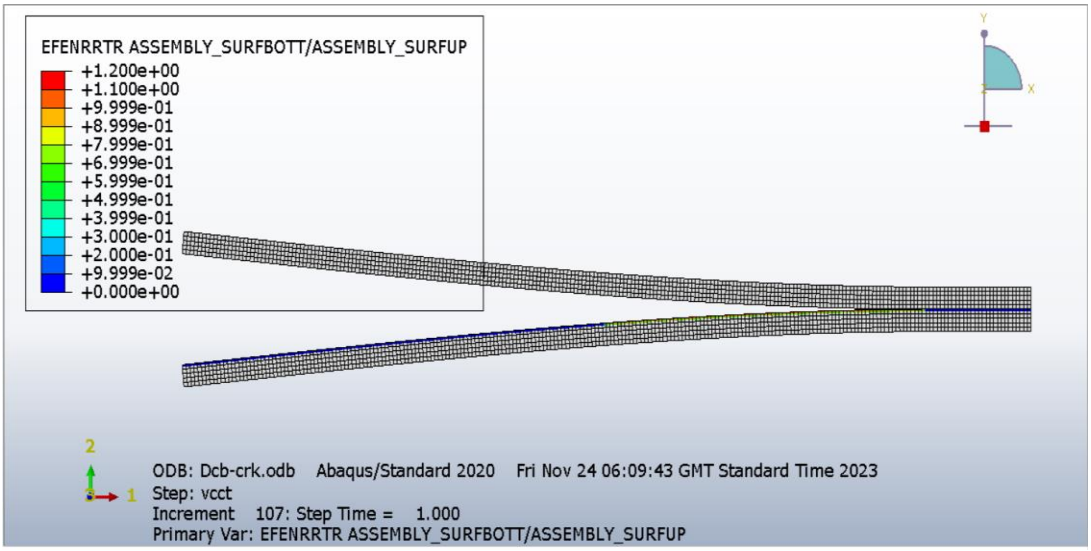

Figure 4.4. The effective strain energy release rate along the crack length.

Figure 4.4 shows that how the strain energy release rate changes as the crack propagates through the material. The strain energy release rate likely starts low and gradually increases as the crack begins to propagate. This indicates that initially, the material resists crack growth. A higher SERR value indicates a more difficult crack to propagate. This suggests that the delamination crack is propagating, and more energy is being required to continue the crack growth as the test progresses.

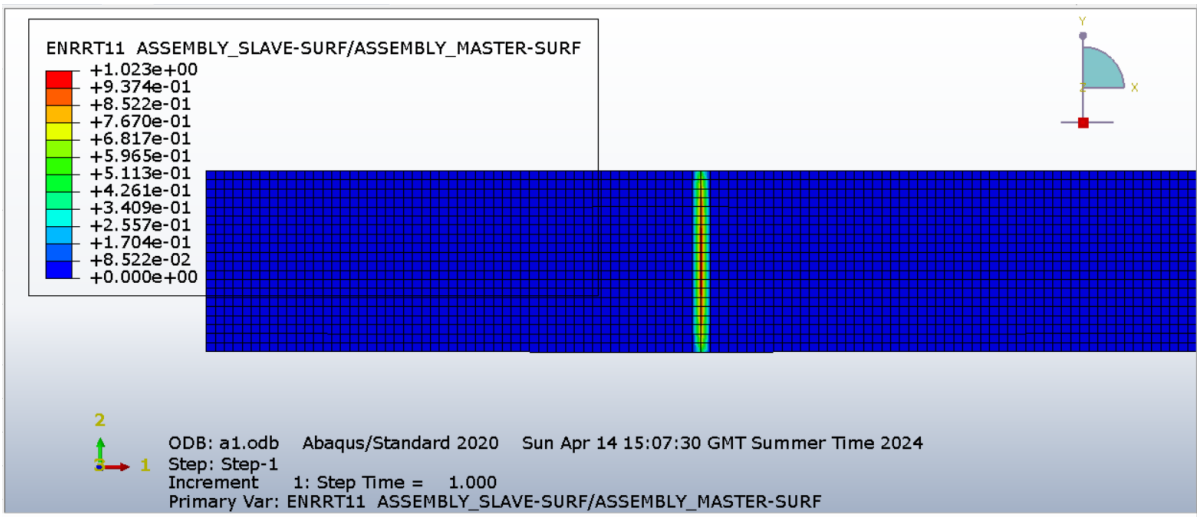

Figure 4.5. $ENRRT_{11}$ along the crack front for the DCB model.

Figure 4.5 shows the strain energy release rate (SERR) $_{11}$ along the crack front for the DCB specimen. In the context of fracture mechanics, a higher SERR indicates a greater ease of crack propagation. The values listed in the image show that there is enough energy for the crack to propagate throughout the entire length simulated.

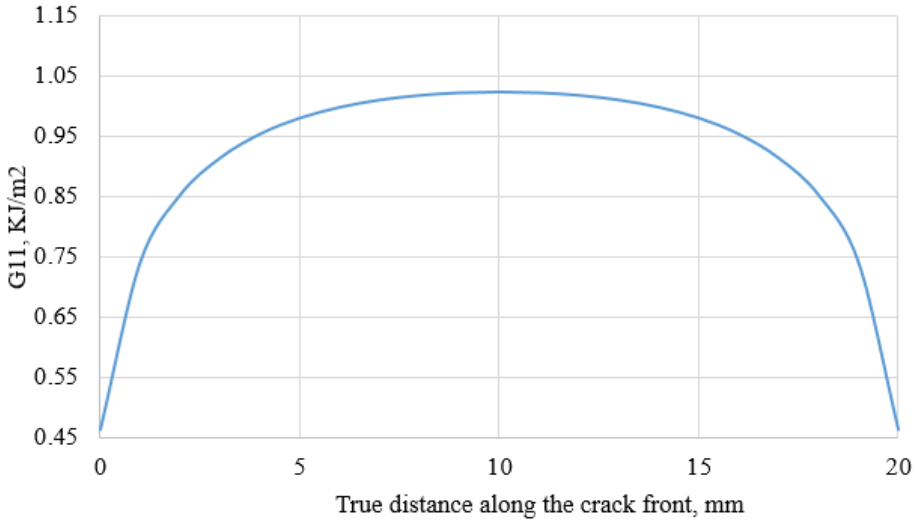

Figure 4.6. Graph of $ENRRT_{11}$ versus crack path along the crack front for the DCB model.

Figure 4.6 shows an upward trend in SERR with increasing time. The specific type of crack this graph represents is a Mode I crack, which is an opening crack. This means the crack faces are moving directly apart from each other. The fact that the values on the y-axis (ENRRT) range from 1.0 to 0.5 suggests that it might represent a normalized value, possibly a relative distance or a scaled energy value. Generally, DCB tests are used to measure the fracture toughness of a material under mode I crack propagation conditions. Fracture toughness is a property of a material that describes its resistance to crack propagation. The results from a DCB test can be used to predict how a crack will propagate in a real structure. The graph likely shows a decrease in stress or strain energy as a crack propagates in a material during a simulated DCB test.

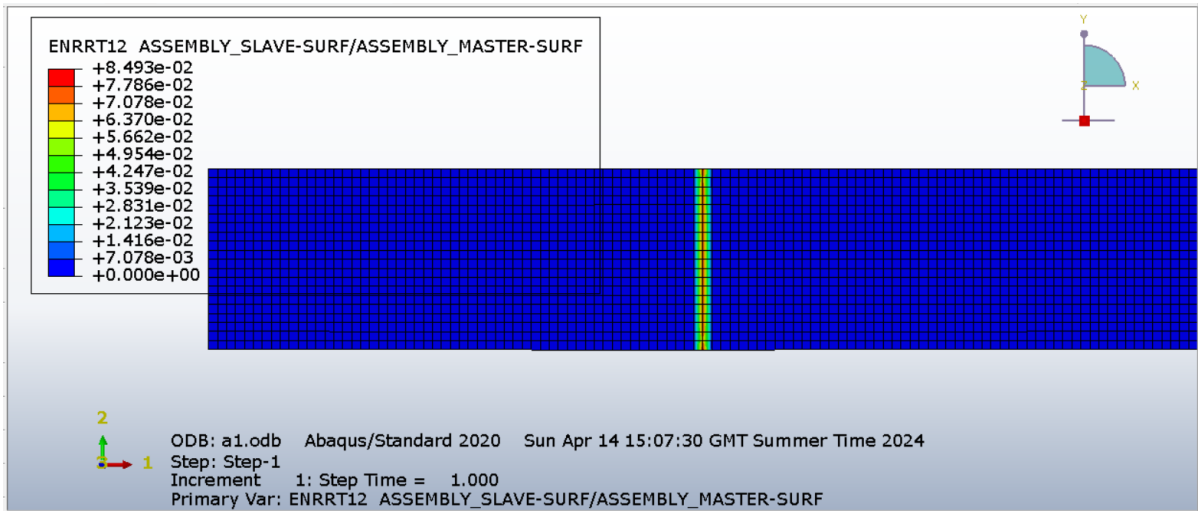

Figure 4.7. $ENRRT_{12}$ along the crack front for the DCB model.

The SERR under Mode I loading is an essential parameter in delamination analysis and its accurate determination is crucial for predicting the delamination behaviour of composite materials under Mode I loading. The strain energy release rate (ENRRT12) in the DCB model varies almost linearly as the front moves through each element.

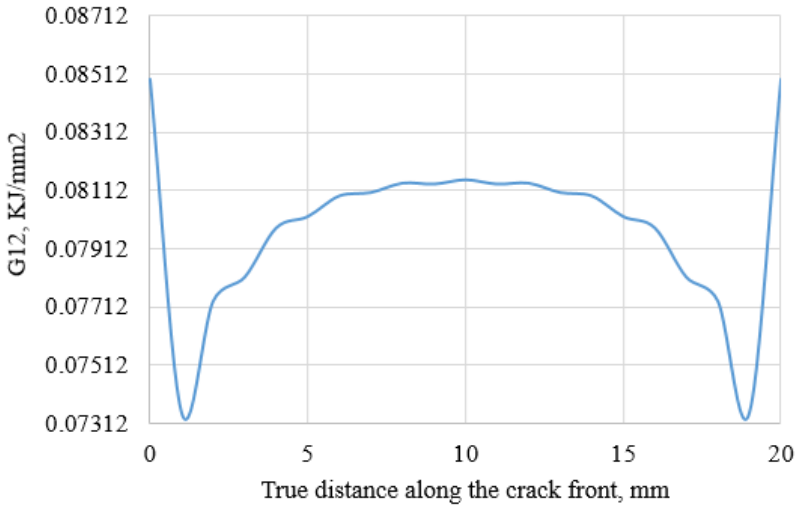

Figure 4.8. Graph of $ENRRT_{12}$ versus crack path along the crack front for the DCB model.

Figure 4.8 shows a general decrease in the ENRRT value as the distance along the crack front increases. This suggests that the value being plotted likely represents a relative quantity that decreases as the distance along the crack path increases. The data plotted in the graph suggests that the strain energy release rate (G) is not constant along the crack front. The total range of G values plotted is about 0.012 KJ/mm², which is a very small variation. It appears to fluctuate slightly as the distance along the crack front increases. This could indicate material inhomogeneity or slight variations in the mesh used in the finite element simulation.

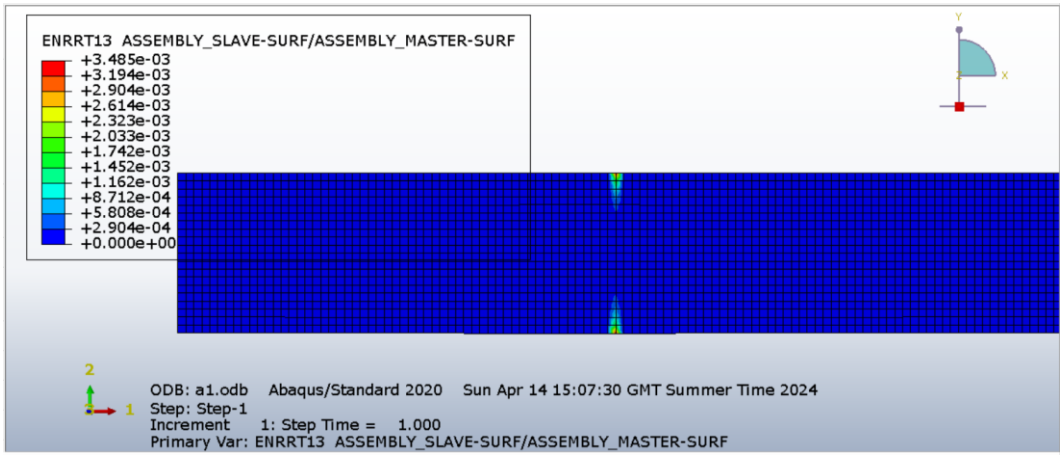

Figure 4.9. $ENRRT_{13}$ along the crack front for the DCB model.

Figure 4.9 shows the visualization of the strain energy release rate required to propagate a crack at different locations along the crack front of a simulated DCB test in Abaqus. The variations in SERR along the crack front could be due to factors like material heterogeneity or the presence of defects. Strain energy release rate is a measure of the energy required to propagate a crack in a material. Higher values indicate more energy is required to grow the crack. +3.485e-03 +3.194e-03 +2.904e-03... shows incremented values that likely represent the position along the crack front where the SERR value was calculated.

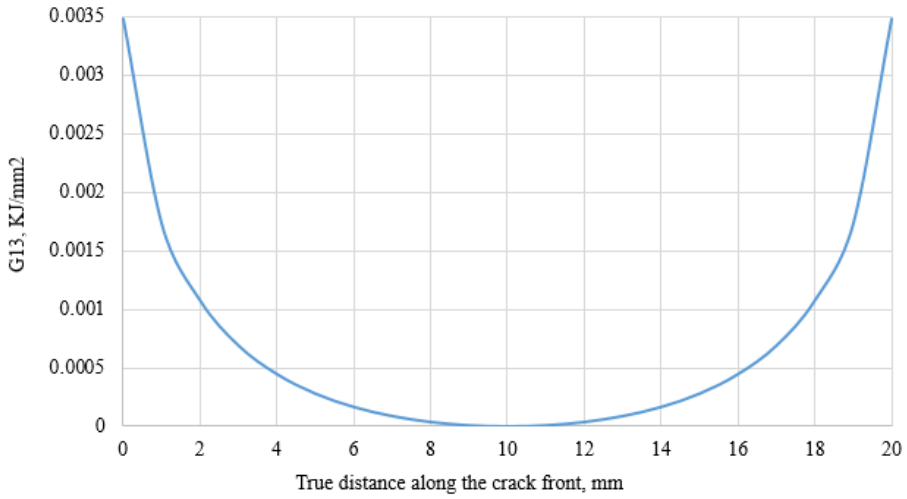

Figure 4.10. Graph of $ENRRT_{13}$ versus crack path along the crack front for the DCB model.

Figure 4.10 shows a general decrease in the strain energy release rate (SERR) as the distance along the crack path increases. The data is from a simulation of a DCB test, which is a common way to measure fracture toughness of a material under mode I crack propagation (crack faces moving directly apart). Given the context of a DCB test and Mode I crack propagation, the decrease in SERR along the crack path suggests that less energy is required to propagate the crack as it grows longer. This can happen for a few reasons. As the crack gets longer, the stress concentration at the crack tip can decrease, making it easier for the crack to grow. Additionally, the material ahead of the crack may have undergone some plastic deformation or damage, making it weaker and easier to fracture. The graph shows a decrease in strain energy release rate (SERR) as a crack propagates in a material during a simulated DCB test

under mode I loading conditions in Abaqus. This suggests that it becomes easier to propagate the crack as it gets longer.

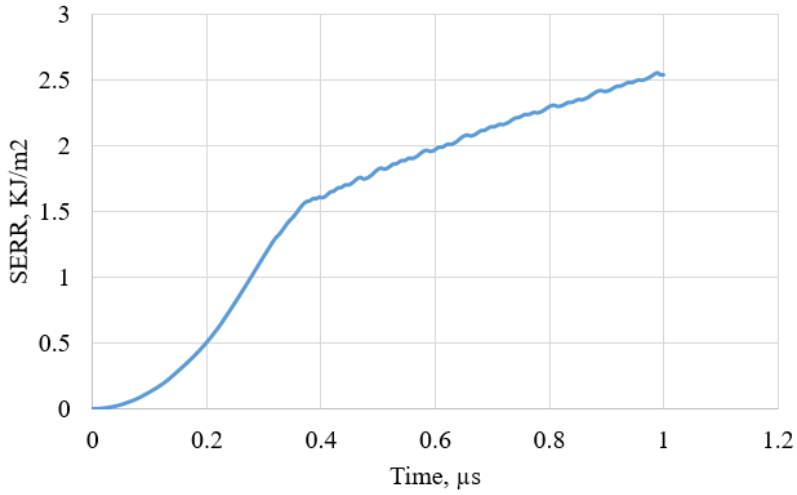

Figure 4.11. Strain-energy release rate versus time graph output for the whole DCB model.

Figure 4.11 represents the SERR for the whole DCB model. A higher SERR value indicates a more difficult crack to propagate. The graph shows an upward trend in SERR with increasing time. This suggests that the delamination crack is propagating, and more energy is being required to continue the crack growth as the test progresses. This is a typical characteristic of delamination tests where the crack faces increasing resistance to crack propagation due to factors like material stiffening or fiber bridging. The initial increase in SERR might be steeper due to the initiation and growth of the delamination crack. The rate of SERR increase might slow down or even plateau after a certain point, if the crack propagation reaches a steady state.

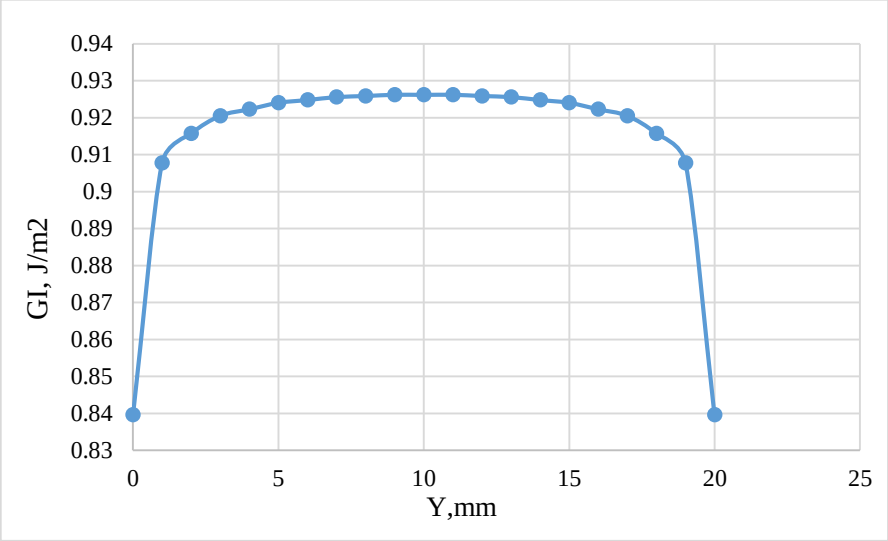

Figure 4.11. The total strain energy release rate along the crack path for Mode I.

Figure 4.11 shows the strain energy release rate (SERR) $_{11}$ along the crack front for the DCB specimen. The graph likely shows a decrease in stress or strain energy as a crack propagates in a material.

The graph reaches a pronounced peak, likely around 0.92 J/m². This represents maximum SERR value for this composite. Beyond this point, the crack requires less energy to propagate, potentially leading to unstable crack growth. The peak value of around 0.92 J/m² indicates a reasonable level of Mode I fracture toughness for this S2 glass/SC15 composite which is less than that of the critical value i.e. 2.5525 J/m².

4.3. Results of ENF delamination with VCCT

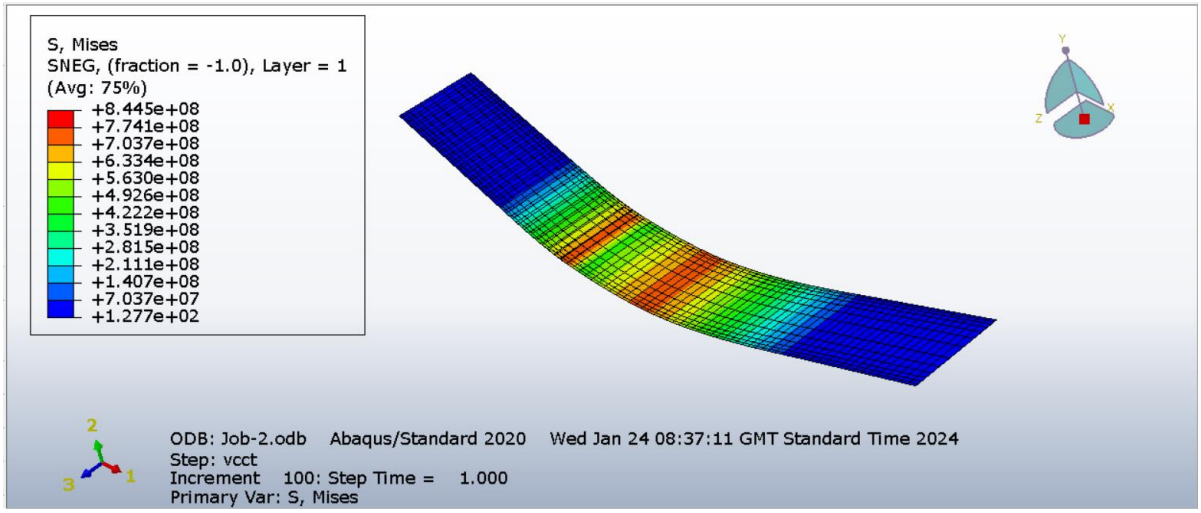

Figure 4.12. Von Mises stresses

Mode II delamination happens when a composite material experiences shear force along the crack plane, causing the layers to slide relative to each other. This is a common failure mode in composites. The simulation shows that the highest stresses are concentrated at the center. The stresses decrease away from the center because the material is able to distribute the load more evenly. The high stresses at the centre in the image are due to the concentration of stress at the notch. The simulation of the von-Mises stress distribution is necessary to identify areas of high stress concentration. Therefore this information is important in designing the material in order to decrease risk of failure.

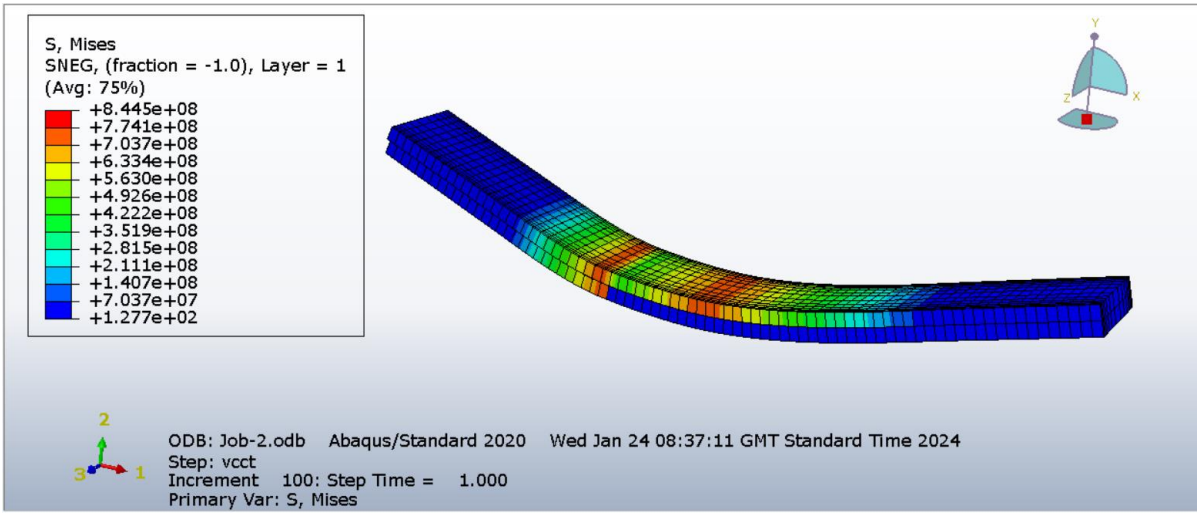

Figure 4.13. View of ENF composite specimen with thickness showing the sliding with an initial crack length of 30mm.

Figure 4.13 shows the image of an ENF simulation under mode II loading with a 30 mm initial crack length would likely show the results of stress distribution and a visible crack with some lateral displacement along the crack faces. Mode II loading refers to a specific type of stress application where there is a shear force acting along the faces of the crack. This can cause the crack to propagate in a direction perpendicular to the applied force. The contour plot showing the distribution of a variable, likely stress, across the geometry of the model. The color legend would indicate high stress (red) and low stress (blue) regions. The colour intensity around the crack tip appears to be higher compared to other areas. This suggests a higher concentration of stress in that region. This is expected because stress tends to concentrate at the tip of cracks. In addition to that the simulation shows that the sliding condition along the initial delamination location tip under mode II loading condition.

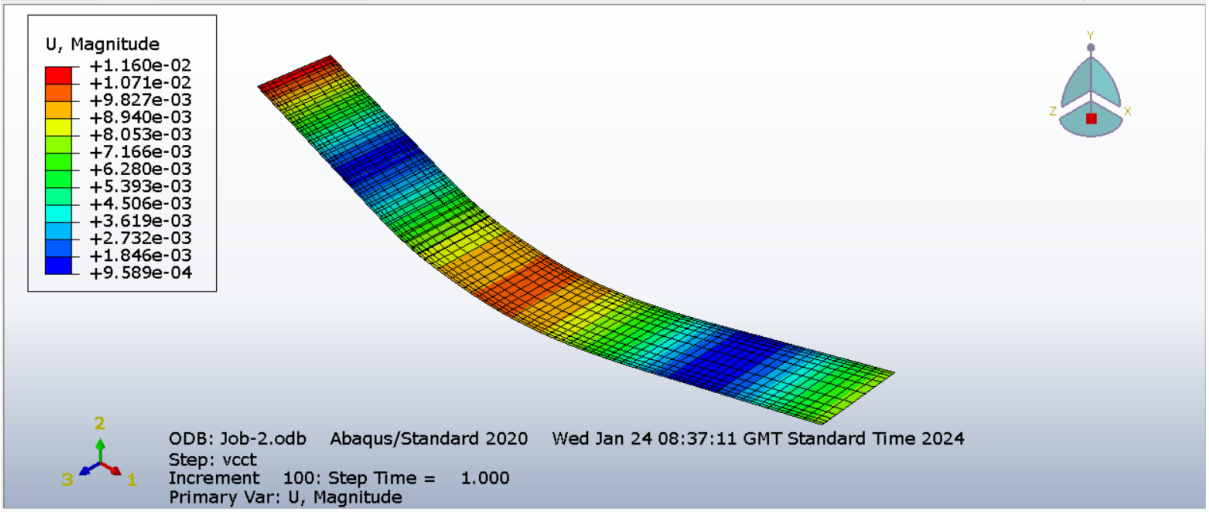

Figure 4.14. Total displacements of ENF specimen.

The End-Notched Flexure (ENF) specimen is a standard test setup to measure Mode II fracture toughness in composites. Its design induces shear forces at a pre-existing crack. The highest stress concentrations are likely to occur near the crack tip and other areas where geometry or loading cause stress build-up. If these stresses exceed the material's strength, delamination will progress.

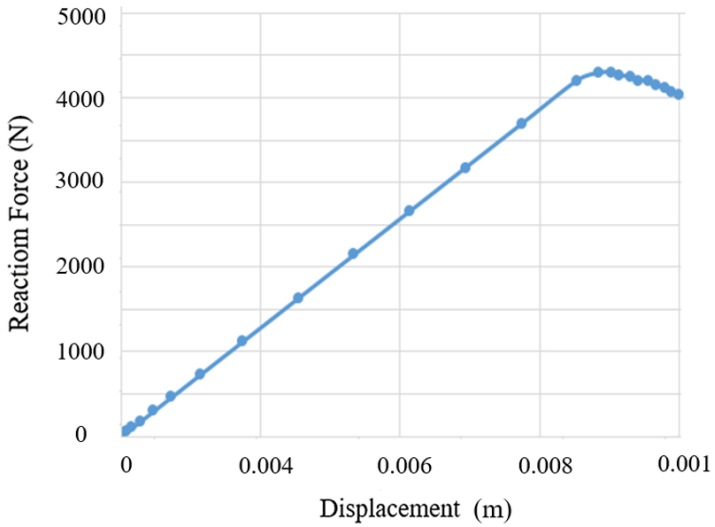

Figure 4.15. Load-displacement graph for mode II delamination.

The delamination begins when the magnitude of the load equals to 4378.26 N and the opening displacement 8.845 mm.

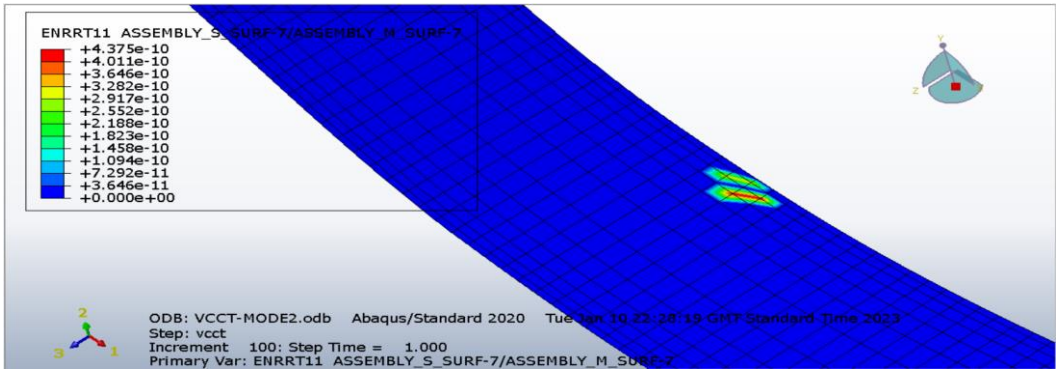

Figure 4.16. The energy release rate at the crack front using VCCT method ($ENRRT_{11}$).

Figure 4.16 shows a plot of the results of a simulation of a crack in a material under shear stress (mode II loading condition). The text labels on the left side of the image show the values of the strain energy release rate (SERR) at different points along the crack path. Strain energy release rate is a measure of the energy available for crack propagation per unit area of new crack surface created. The higher the SERR, the easier it is for the crack to propagate. The simulation was done using the virtual crack closure technique (VCCT). VCCT is a numerical method that is used to calculate the SERR in fracture mechanics simulations. Overall, the image shows the results of a simulation of a crack in a material under shear stress. The simulation shows that the SERR is highest at the beginning of the crack path and then decreases gradually as the crack propagates. This suggests that the material is more resistant to crack propagation at the beginning of the crack path.

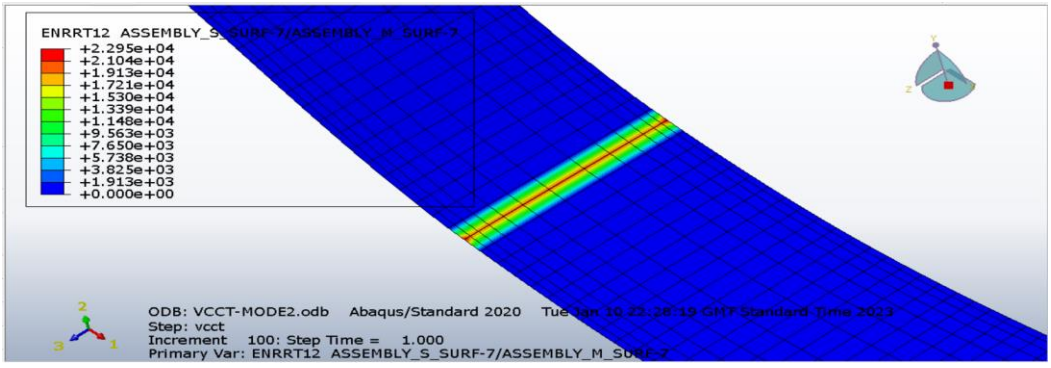

Figure 4.17. The energy release rate at the crack front using VCCT method ($ENRRT_{12}$).

As shown in Figure 4.17 the reddish area in the center of the crack front suggests the primary region where crack propagation is most likely to occur due to the highest concentration of SERR. The slightly higher SERR on the right side aligns with the 0-degree fibers in the [0/90/0/90] s layup. This asymmetry could be attributed to the stronger resistance offered by these fibers against shear compared to the 90-degree fibers on the left side.

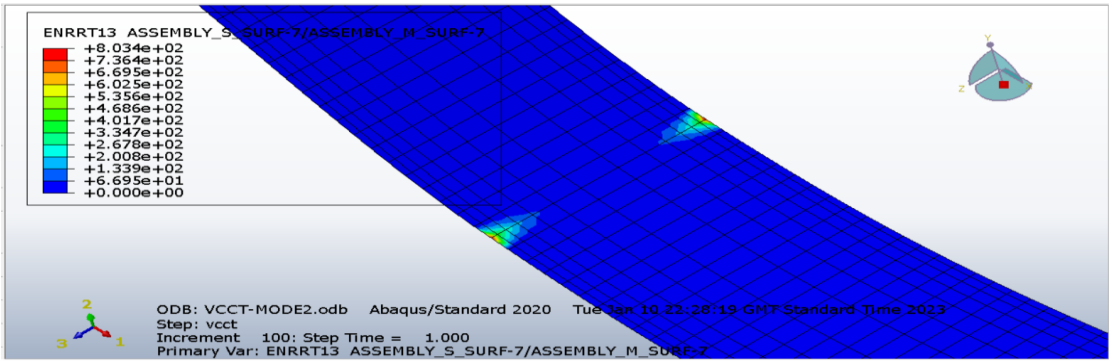

Figure 4.18. The energy release rate at the crack front using VCCT method ($ENRRT_{13}$).

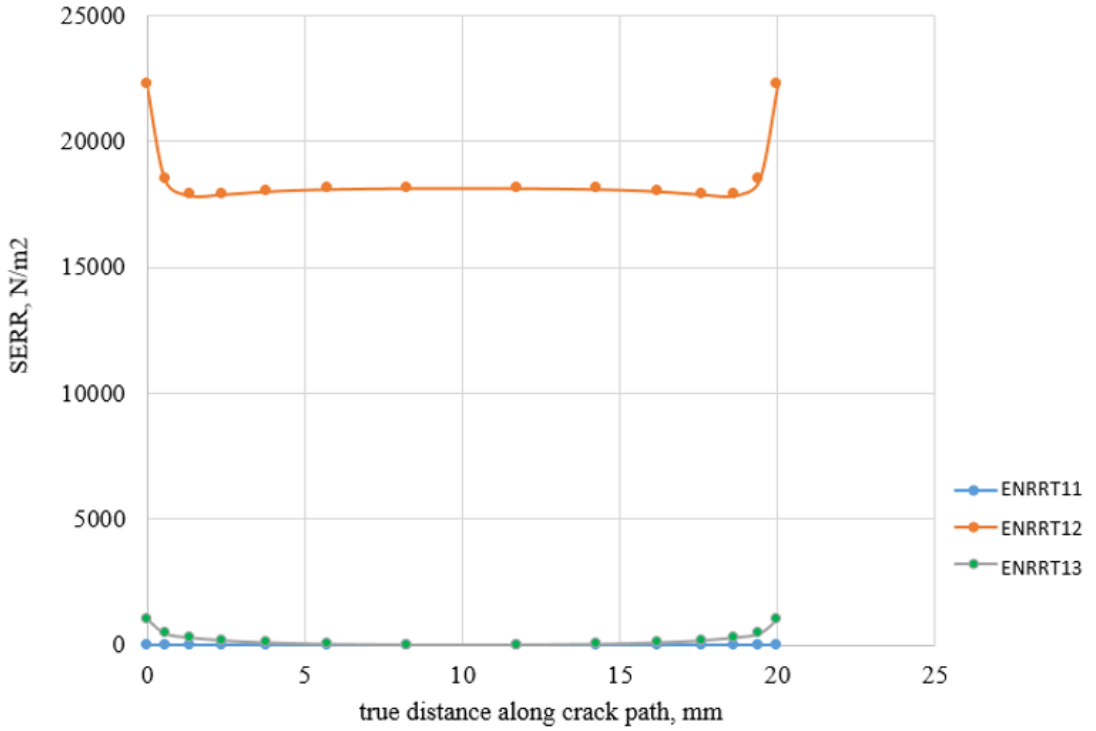

Figure 4.19. The three $ENRRT_{along}$ the crack front.

Figure 4.19 shows the true distance along the path versus the energy for an ENF specimen subjected to three-point bending. The graph shows a non-linear relationship between the true distance along the path and the energy. This is because the fracture toughness increases with crack length. The x-axis of the plot is likely the distance along the crack path, and the y-axis is the SERR. The curve shows that the SERR is highest at the beginning of the crack path and then decreases gradually as the crack propagates. This suggests that the material is more resistant to crack propagation at the beginning of the crack path.

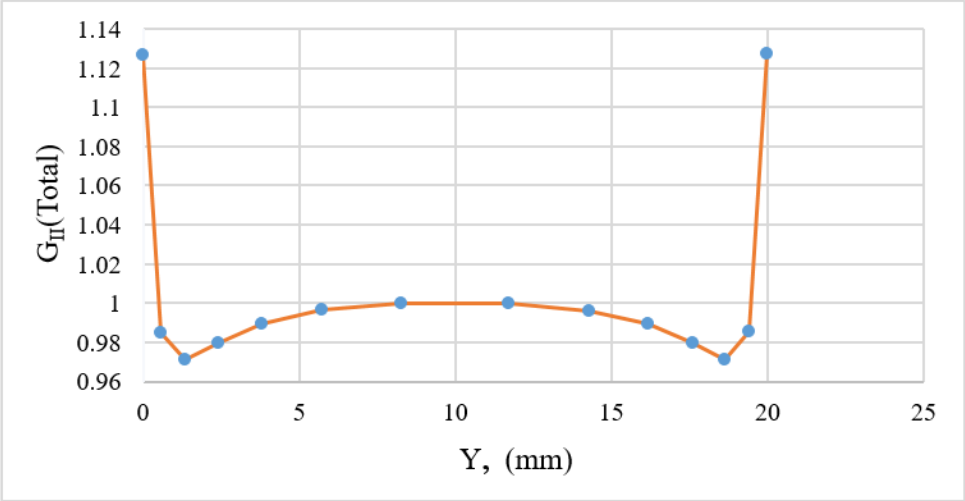

Figure 4.20. The total strain energy release rate along the crack path.

Figure 4.20 shows how the total SERR changes as the crack propagates. The analysis begins with a 30mm pre-existing crack. The SERR starts relatively low and increases steadily when crack begins to propagate. This is typical as the material resists the shear forces during the initial stages of crack growth. The graph reaches a pronounced peak, likely around 1.1 J/m². This represents maximum SERR value for this composite. Beyond this point, the crack requires less energy to propagate, potentially leading to unstable crack growth. The peak value of around 1.1 J/m² indicates a reasonable level of Mode II fracture toughness for this S2 glass/SC15 composite.

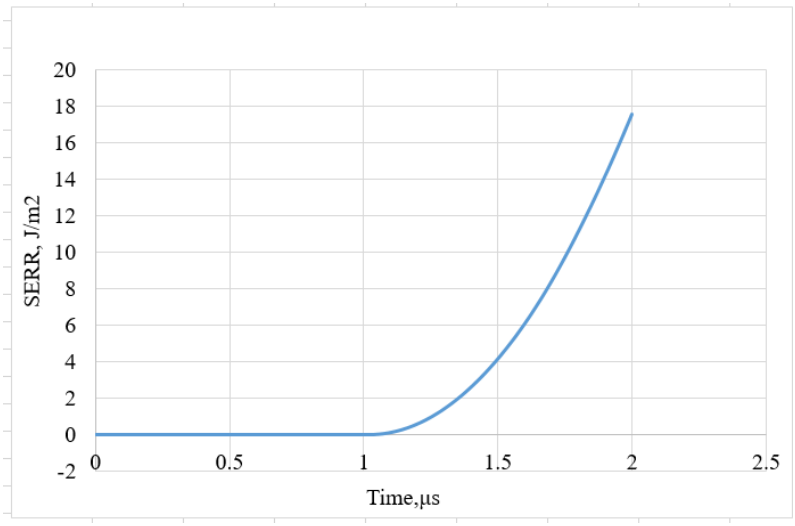

Figure 4.21. Strain-energy release rate versus time graph output for the whole DCB model.

Figure 4.21 shows a general upward trend in SERR with increasing time. This indicates that as the crack propagates in the ENF model, the material offers increasing resistance to the crack growth. This is a common observation in delamination tests where factors like material stiffening or fiber bridging hinder the crack propagation. There seems to be a steeper increase in SERR at the beginning (around the initial 1.2 microseconds). This could be attributed to the initial crack initiation and growth phase.

4.4. Validation

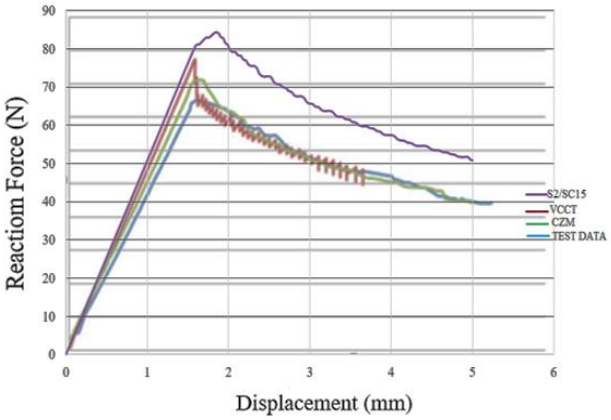

Figure 4.22. Comparison of delamination result of S2glass/SC15 composite under Mode I loading (DCB) with the literature. [54]

Figure 4.22 compares the result of S2 glass fiber/ SC15 epoxy composite material fracture analysis with literature data (Delamination of C/PEKK I-Beam using virtual crack closure technique and cohesive zone method by Greeshma Ramakrishna)[54] of VCCT (Virtual Crack Closure Technique), CZM (Cohesive Zone Model), and test data for a DCB (Double Cantilever Beam) interlaminar fracture test.

The VCCT results for S2/SC15 epoxy composite are significantly higher than all the literature data. This suggests that the VCCT method predicts a higher force required to cause a crack to propagate in the material than either the CZM method or the materials tested in the referenced literature.

There are a couple of reasons why this might be the case. VCCT is generally considered to be a more accurate method for modelling crack propagation than CZM. CZM uses a simpler approach to model the material behaviour ahead of the crack tip, whereas VCCT takes into account the actual closure of the crack surfaces behind the crack tip. This can lead to more accurate predictions of the force required to propagate the crack.

Additionally, the accuracy of the results from both VCCT and CZM can be affected by the specific material properties that are input into the model. It is possible that the material properties used in the Abaqus simulation were different from the materials tested in the literature data. This could also explain the discrepancy between the results.

Overall, the graph suggests that the VCCT method provides a more accurate prediction of the force required to cause crack propagation in the DCB specimen than the CZM method. However, the results are still higher than the literature data, which could be due to differences in material properties.

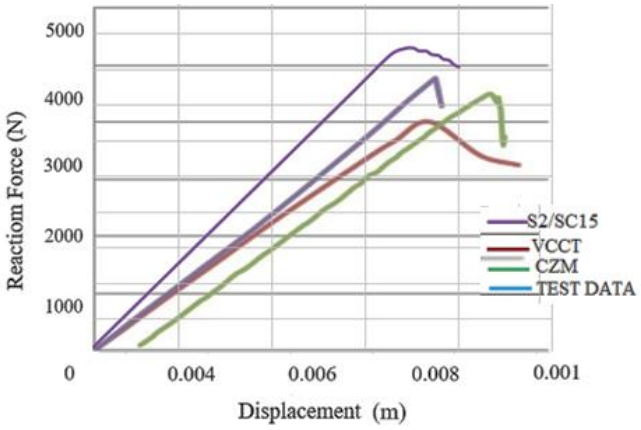

Figure 4.23. Comparison of delamination result of Sw2glass/SC15 composite under Mode II loading (ENF) with the literature. [54]

Figure 4.23 compares the results of an Abaqus interlaminar fracture analysis using VCCT (Virtual Crack Closure Technique) on ENF (End Notched Flexure) with literature data.

The VCCT results appear to be consistent with the literature data. Both datasets show a similar trend of increasing force with increasing displacement. This suggests that the Abaqus simulation using VCCT is capturing the real-world behaviour of the material being tested which suggests that the VCCT analysis is providing a reasonable prediction of the force required to cause a crack to propagate in the ENF specimen.

Chapter Five

5. Conclusion and Recommendation

5.1. Conclusion

In this study, a numerical analysis of DCB and ENF specimens were performed to investigate delamination in S2 glass/SC15 epoxy composite which has a fire retarding behavior under Mode I and Mode II loading conditions using Abaqus. The crack pattern was studied using the VCCT method with a two-dimensional model of the specimens, providing valuable insights into the interlaminar fracture behavior and mechanical properties of the composite material.

The simulation of the DCB and ENF tests was carried out using ABAQUS software to demonstrate delamination. The results indicated that the S2 glass/SC15 epoxy composite exhibited good mechanical properties, with both the ENF and DCB tests showing high levels of fracture toughness. This suggests that the S2 glass/SC15 epoxy composite is a suitable choice for applications requiring high strength and toughness in vehicle industries. By utilizing the simulation findings, the composite design can be optimized and its performance enhanced in various applications.

Through the determination of the strain energy release rate and analysis of force-displacement graphs, significant findings were obtained. The study successfully characterized the delamination behavior of the composite laminate under both Mode I and Mode II loading, providing insights into its fracture mechanics properties. The investigation into the strain energy release rate offered a quantitative measure of the energy required for crack propagation, aiding in understanding the material's resistance to delamination.

The DCB delamination begins when the magnitude of the load equals to 83.4477 N and the opening displacement 1.794 mm. In case of ENF delamination begins when the magnitude of the load equals to 4378.26 N and the opening displacement 0.0094 m. The G_{IC} value 1.1kJ/m² indicates a reasonable level of fracture toughness for S2 glass/SC15 composite.

5.2. Recommendation

There are several potential areas for future work to further understand composite material characteristics. The simulation can be extended to include mixed-mode delamination propagation, which is more representative of real-world composite structures. This can be achieved by applying CZM or other fracture mechanics approaches.

In addition, investigating composite material behavior under fatigue and cyclic loading conditions is crucial for predicting the durability of composite structures. This can be done by simulating the tests under various loading cycles and evaluating the propagation of the crack.

The effects of temperature and environmental conditions on the composite material's properties and behavior can also be studied. This can help in understanding the capacity of the composite under different operating conditions and may be performed by simulating the tests at various temperatures and humidity levels.

Furthermore, investigating the composite behavior under impact and high-speed loading conditions, which are relevant for many engineering applications, can be done by simulating the tests using explicit dynamics analysis and evaluating the crack growth under these loading conditions.

Future works can be titled as:

- ✓ Fractural analysis of S2glass/ SC15 epoxy plain woven composite using cohesive zone modeling
- ✓ Fractural analysis of S2glass/ SC15 epoxy plain woven composite under thermal effect using FEM
- ✓ Fractural analysis of S2glass/ SC15 epoxy plain woven composite under fatigue loading condition using FEM
- ✓ Mixed-mode delamination behaviour of S2glass/ SC15 epoxy plain woven composite under impact loading using FEM
- ✓ Fractural behaviour of S2glass/ SC15 epoxy plain woven composite under high speed loading condition using FEM

References

[1] B. N. Swamy, C. Lakshmaiah, and K. T. Reddy, "Modeling and Analysis of Light Vehicle Chassis Made of Composite Material," vol. 7, no. 3, pp. 5011–5015, 2017.

[2] K. Saravanakumar, V. Arumugam, R. Souhith, and C. Santulli, "Influence of milled glass fiber fillers on mode I & mode II interlaminar fracture toughness of epoxy resin for fabrication of glass/epoxy composites," *Fibers*, vol. 8, no. 6, 2020, doi: 10.3390/FIB8060036.

[3] T. P. Sathishkumar, S. Satheeshkumar, and J. Naveen, "Glass fiber-reinforced polymer composites - A review," *J. Reinf. Plast. Compos.*, vol. 33, no. 13, pp. 1258–1275, 2014, doi: 10.1177/0731684414530790.

[4] N. Jesuarockiam, "Journal of Reinforced," no. June, 2014, doi: 10.1177/0731684414530790.

[5] T. Grover, A. Khandual, K. N. Chatterjee, and R. Jamdagni, "TEXTILE POT POURI Flame retardants : An overview," no. December, pp. 29–36, 2015.

[6] M. Thesis, "Modeling of Long-Fiber-Reinforced Composites in ABAQUS," no. October, 2014.

[7] E. Mfoumou and S. Kao-Walter, "Fracture Toughness Testing of Non Standard Specimens,"2004,[Online].Available: http://www.bth.se/fou/Forskinfo.nsf/0/bacf1176dfbe0526c1256e7b0027fd60/$file/Res_rep_200405.pdf.

[8] H. T. Hu, W. P. Lin, and F. T. Tu, "Failure analysis of fiber-reinforced composite laminates subjected to biaxial loads," *Compos. Part B Eng.*, vol. 83, pp. 153–165, 2015, doi: 10.1016/j.compositesb.2015.08.045.

[9] P. M. Stress, "Stress Intensity Factor," *Encycl. Therm. Stress.*, pp. 4613–4613, 2014, doi: 10.1007/978-94-007-2739-7_100614.

[10] S. Y. Degefe and D. Tilahun, “Finite Element Analysis of E-glass / Epoxy Composite for Automotive Structures Thesis By : Advisor : Finite Element Analysis of E-glass / Epoxy Composite for Automotive Structures,” 2015.

[11] R. Rikards, “Interlaminar fracture behaviour of laminated composites,” vol. 76, 2000.

[12] “Parte I Anderson T.L. Fracture mechanics - Fundamentals and applications.pdf.” .

[13] A. Mohamadi, M. Behnia, and M. Alneasan, “Comparison of the classical and fracture mechanics approaches to determine in situ stress/hydrofracturing method,” *Bull. Eng. Geol. Environ.*, vol. 80, no. 5, pp. 3833–3851, 2021, doi: 10.1007/s10064-021-02184-8.

[14] P. Hvizdoš, P. Tatarko, A. Duszova, and J. Dusza, *Failure mechanisms of ceramic nanocomposites*. 2013.

[15] A. Of, “O N -L Ine a Ppendix B :,” pp. 1–13.

[16] M. F. Kanninen, C. H. Popelar, and A. J. McEvily, *Advanced Fracture Mechanics*, vol. 108, no. 2. 1986.

[17] O. E. Okay, “No Title,” *Int. J. Dev. Manag. Rev.*, vol. 5, no. 1, pp. 212–224, 2010, [Online].Available: http://publications.lib.chalmers.se/records/fulltext/245180/245180.pdf%0Ahttps://hdl.handle.net/20.500.12380/245180%0Ahttp://dx.doi.org/10.1016/j.jsames.2011.03.003%0Ahttps://doi.org/10.1016/j.gr.2017.08.001%0Ahttp://dx.doi.org/10.1016/j.precamres.2014.12.

[18] “LINEAR ELASTIC.”

[19] D. W. Hoffman, “No Title,” pp. 4–7.

[20] S. Edition, *MECHANICS OF*. 1999.

[21] “Classification of composites,” no. Mmc.

[22] R. Kitey, K. Chawla, and R. Kitey, “ScienceDirect ScienceDirect ScienceDirect

Interlaminar Fracture Toughness of Short Fibre Reinforced GFRP Interlaminar Fracture Toughness of Short Fibre Reinforced GFRP Laminates Thermo-mechanical a high pressure turbine blade of an airplane gas turbine en," *Procedia Struct. Integr.*, vol. 14, no. 2018, pp. 571–576, 2019, doi: 10.1016/j.prostr.2019.05.070.

[23] B. Jones, K. Thanapalan, and E. Constant, "Fracture toughness prediction of composite materials," *2019 6th Int. Conf. Control. Decis. Inf. Technol. CoDIT 2019*, pp. 1870–1875, 2019, doi: 10.1109/CoDIT.2019.8820438.

[24] M. Schober, "On the Characterization and Modeling of Interfaces in Fiber Reinforced Polymer Structures," p. 175, 2019.

[25] P. Wriggers and G. Zavarise, *Lecture Notes in Applied and Computational Mechanics: Preface*, vol. 58 LNACM. 2011.

[26] T. Jarvie, "Crack Tip Opening Displacement," *White Pap. Stork Mater. Technol.*, p. 8, 2011, [Online]. Available: https://www.scribd.com/document/245778425/Crack-Tip-Opening-Displacement-WPHead.

[27] R. Krueger, *The virtual crack closure technique for modeling interlaminar failure and delamination in advanced composite materials*. Elsevier Ltd., 2015.

[28] ASTM D5528-01, "Standard test method for mode I interlaminar fracture toughness of unidirectional fiber-reinforced polymer matrix composites," *Am. Stand. Test. Methods*, vol. 03, no. Reapproved 2007, pp. 1–12, 2014, doi: 10.1520/D5528-01R07E03.2.

[29] ASTM D7905, "Standard test method for determination of the mode II interlaminar fracture toughness of unidirectional fiber-reinforced polymer matrix composites," *Astm*, pp. 1–18, 2014, doi: 10.1520/D7905.

[30] M. S. S. Prasad, C. S. Venkatesha, and T. Jayaraju, "Experimental Methods of Determining Fracture Toughness of Fiber Reinforced Polymer Composites under Various Loading Conditions," vol. 10, no. 13, pp. 1263–1275, 2011.

[31] B. Pipes, "Interlaminar Fracture of Composite Materials," no. September 1982, 2017,

doi: 10.1177/002199838201600503.

[32] H. Jung and Y. Kim, “Mode I fracture toughness of carbon-glass / epoxy interply hybrid composites †,” vol. 29, no. 5, pp. 1955–1962, 2015, doi: 10.1007/s12206-015-0416-3.

[33] A. Korjakin and R. Fukards, “of GFRP With Different Fiber Surface Treatments,” vol. 19, no. 6, pp. 793–806.

[34] V. Prasad, K. Sekar, S. Varghese, and M. A. Joseph, “Enhancing Mode I and Mode II interlaminar fracture toughness of fl ax fi bre reinforced epoxy composites with nano TiO 2,” *Compos. Part A*, vol. 124, no. June, p. 105505, 2019, doi: 10.1016/j.compositesa.2019.105505.

[35] “Computational Micromechanics Models for Damage and Fracture of Fiber-Reinforced Polymers,” 2018.

[36] M. Jawaid, “Durability and Life Prediction in Biocomposites, Fibre-Reinforced Composites and Hybrid Composites,” no. October, 2018, doi: 10.1016/B978-0-08-102290-0.00007-6.

[37] D. Rakshit and S. Chakraborty, “Determination of fracture parameters of FRP composites : A combined experimental and numerical investigation,” 2013, doi: 10.1177/0021998313516142.

[38] M. A. Fentahun, P. Mahmut, and A. Savaş, “Materials Used in Automotive Manufacture and Material Selection Using Ashby Charts,” vol. 8, no. 3, pp. 40–54, 2018, doi: 10.5923/j.ijme.20180803.02.

[39] Eric A. Nyberg, “Lightweight Materials R&D Program-Annual Progress Report,” 2013,[Online].Available: https://www.energy.gov/sites/prod/files/2014/04/f15/2013_lightweight_materials_apr.pdf.

[40] T. Edition, *FIBER- REINFORCED*. 2007.

[41] M. Müller, P. Valášek, and L. Tomek, "Mechanical properties of polymeric particle composites," *Conf. Proceeding - 4th Int. Conf. TAE 2010 Trends Agric. Eng. 2010*, pp. 454–458, 2010.

[42] C. Edwards, "Influence of Material Selection and Fabrication Process Repeatability on Mechanical Properties of Glass-Polymer Matrix Composite Structures," 2011.

[43] L. J. Deka, S. D. Bartus, and U. K. Vaidya, "Multi-site impact response of S2-glass / epoxy composite laminates," *Compos. Sci. Technol.*, vol. 69, no. 6, pp. 725–735, 2009, doi: 10.1016/j.compscitech.2008.03.002.

[44] T. Abaqus, "Abaqus," pp. 1–6, 1978.

[45] "ABAQUS/CAE is the Complete ABAQUS Environment that provides a," p. 5513, 2009.

[46] Dassault Systèmes Simulia, "Getting Started With ABAQUS Inactive Edition Version 6.8," pp. 1–621, 2008.

[47] K. Song, C. Davila, and C. Rose, "Guidelines and parameter selection for the simulation of progressive delamination," *2008 ABAQUS User's Conf.*, pp. 1–15, 2008, [Online]. Available: http://www.simulia.com/forms/world/pdf2008/SONG-AUC2008.pdf.

[48] B. V. kumar and Y. V. Babu, "An Investigation of Ply Behavior in A GFRP Composite Laminated Plate," *Int. J. Innov. Res. Sci. Eng. Technol.*, vol. 03, no. 11, pp. 17341–17350, 2014, doi: 10.15680/ijirset.2014.0311036.

[49] D. K. Y. Tam, S. Ruan, P. Gao, and T. Yu, "High-performance ballistic protection using polymer nanocomposites," *Adv. Mil. Text. Pers. Equip.*, pp. 213–237, 2012, doi: 10.1533/9780857095572.2.213.

[50] E. Library, "Energy Concepts for Crack Growth | Engineering Library," pp. 1–10, 1996, [Online].Available:https://engineeringlibrary.org/reference/fracture-mechanics-energy-concepts-for-crack-growth.

[51] Sengupta, “Working Stress and Failure Theories A Simplified Approach,” *Stress Int. J. Biol. Stress*, pp. 1–8, 2005.

[52] E. Polyzos, D. Van Hemelrijck, and L. Pyl, “An Open-Source ABAQUS Plug-In for Delamination Analysis of 3D Printed Composites,” *Polymers (Basel).*, vol. 15, no. 9, pp. 1–19, 2023, doi: 10.3390/polym15092171.

[53] L. Banks-Sills, J. Aboudi, R. Eliasi, V. Fourman, and L. Rogel, “Delamination tests of DCB specimens composed of woven composites,” *EPJ Web Conf.*, vol. 6, no. 8872, pp. 3–4, 2010, doi: 10.1051/epjconf/20100642007.

[54] G. Ramakrishna, “Delamination of C / PEKK I-Beam using virtual crack closure technique and cohesive zone method,” 2015, [Online]. Available: https://docs.lib.purdue.edu/open_access_theses/599/.

Appendixes

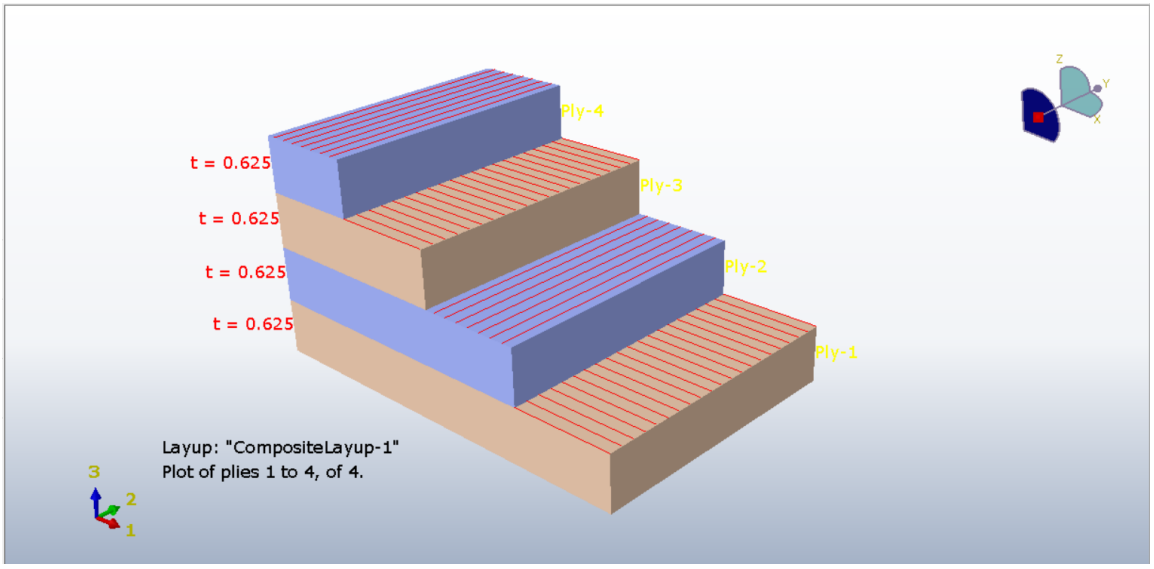

Figure 1. Composite lay-up stacking sequence for symmetry model of DCB.

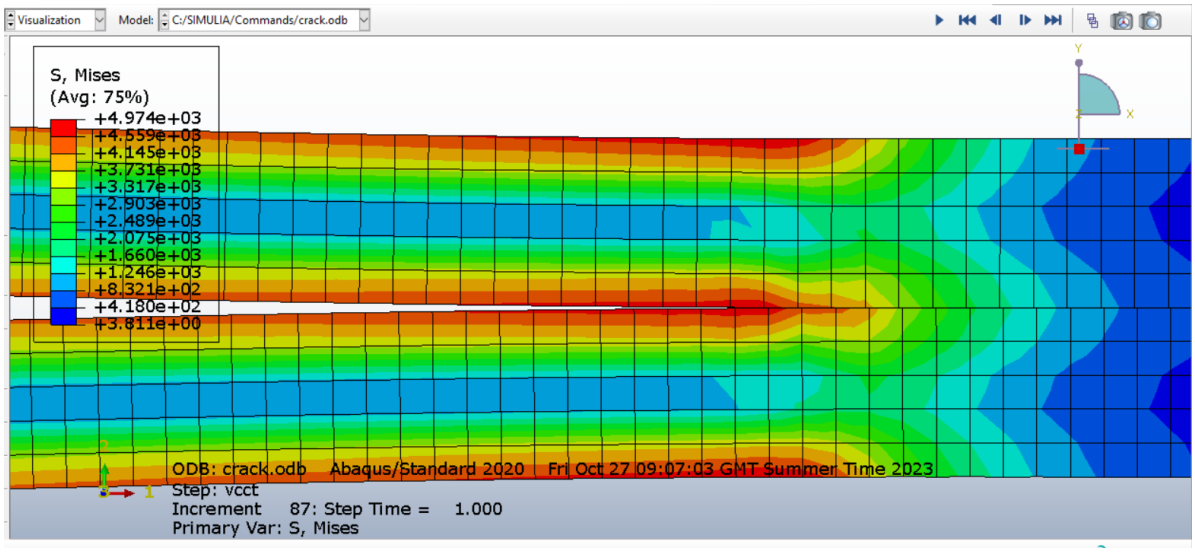

Figure 2. Closest view of stress concentration nearest the crack tip of DCB.

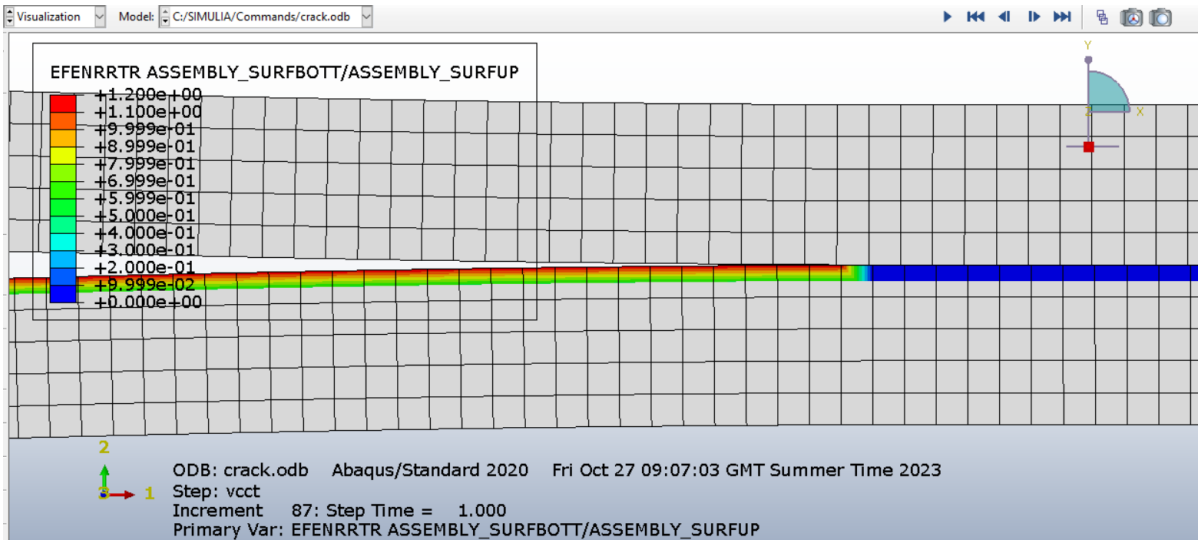

Figure 3. The closest view of strain energy release rate along the crack length of DCB.

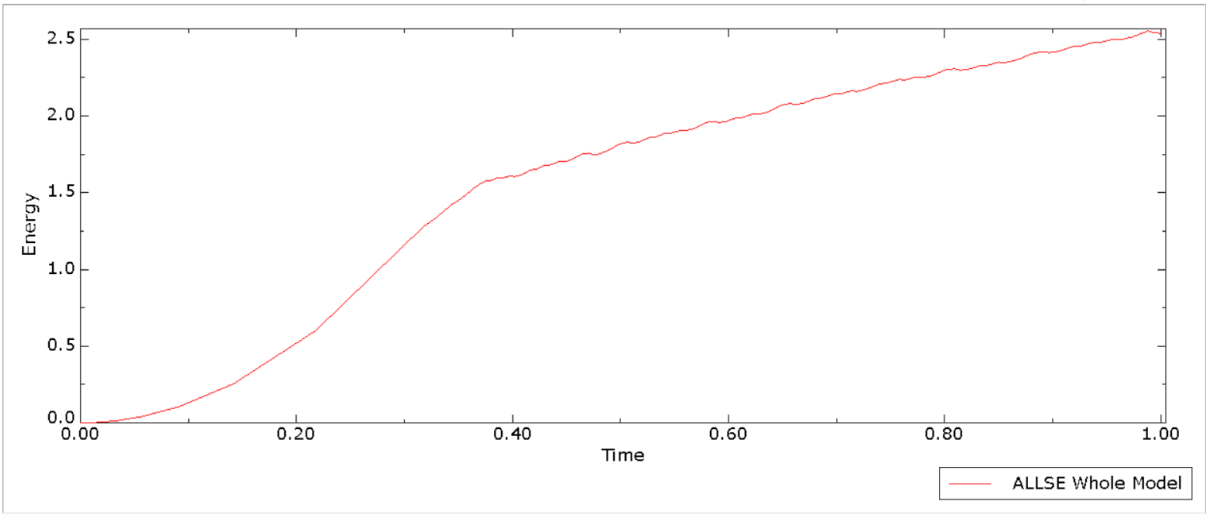

Figure 4. Strain-energy release rate versus time graph Abaqus result for the DCB model.

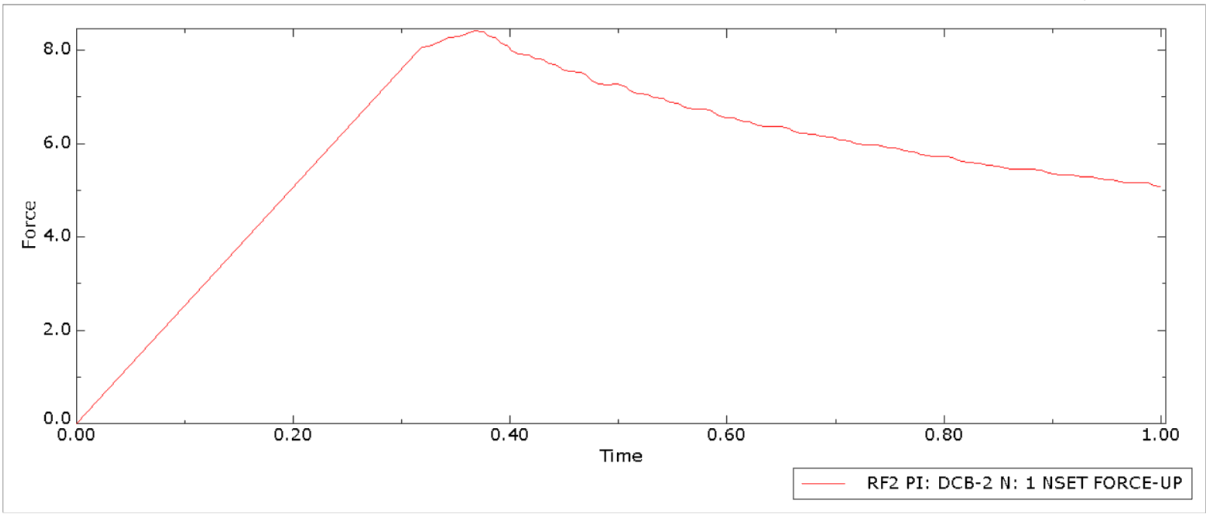

Figure 5. Force-displacement graph of the DCB model from the Abaqus simulation result.

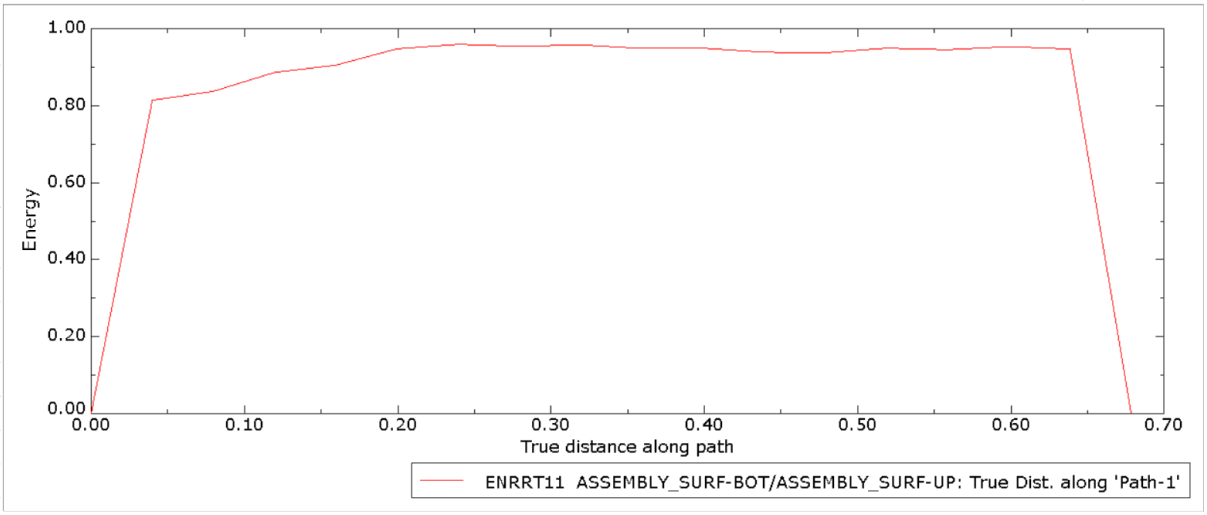

Figure 6. Abaqus result showing the energy release rate $ENRRT_{11}$ along the crack length for DCB simulation.

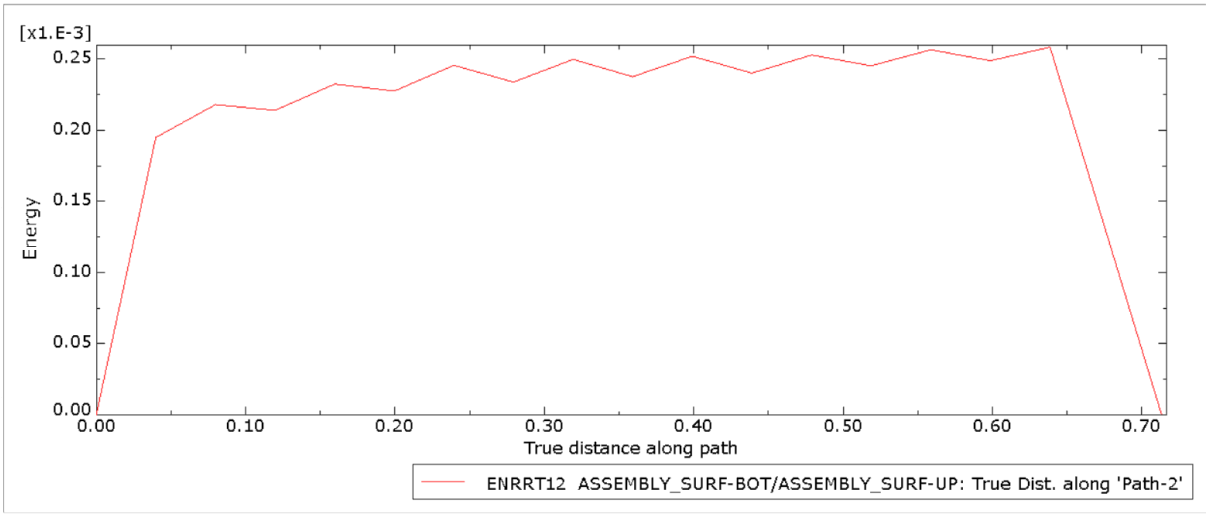

Figure 7. Abaqus result showing the energy release rate $ENRRT_{12}$ along the crack path for DCB simulation.

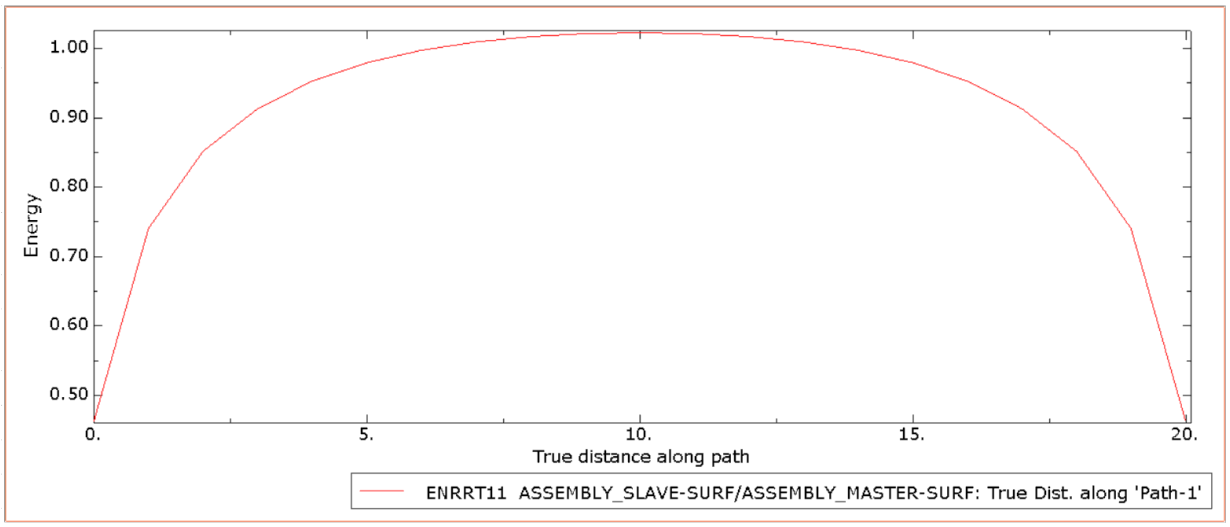

Figure 8. Graph of $ENRRT_{11}$ versus crack path along the crack front for the DCB model.

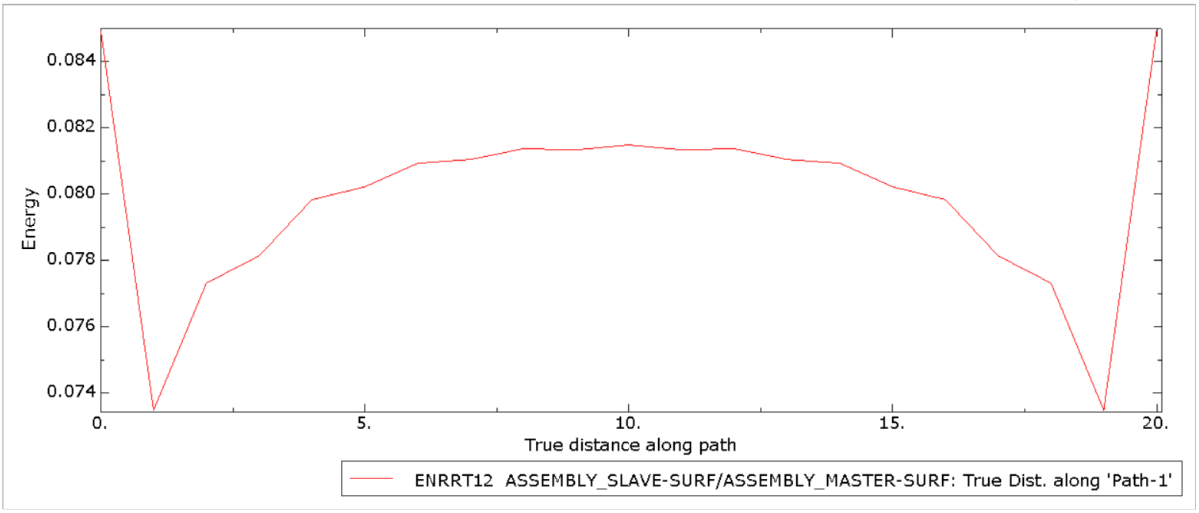

Figure 9. Graph of $ENRRT_{12}$ versus crack path along the crack front for the DCB model.

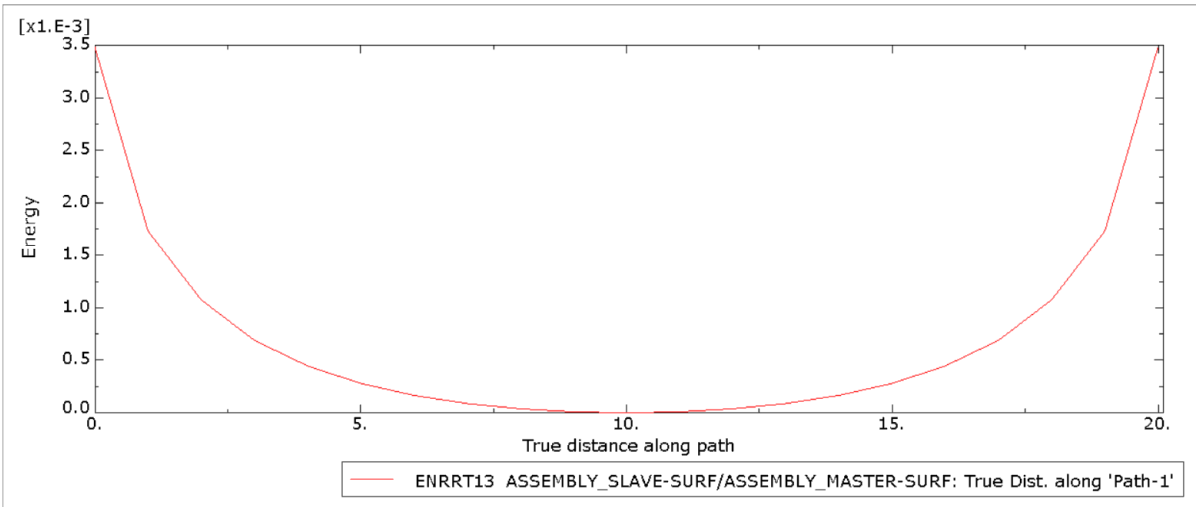

Figure 10. Graph of $ENRRT_{13}$ versus crack path along the crack front for the DCB model.

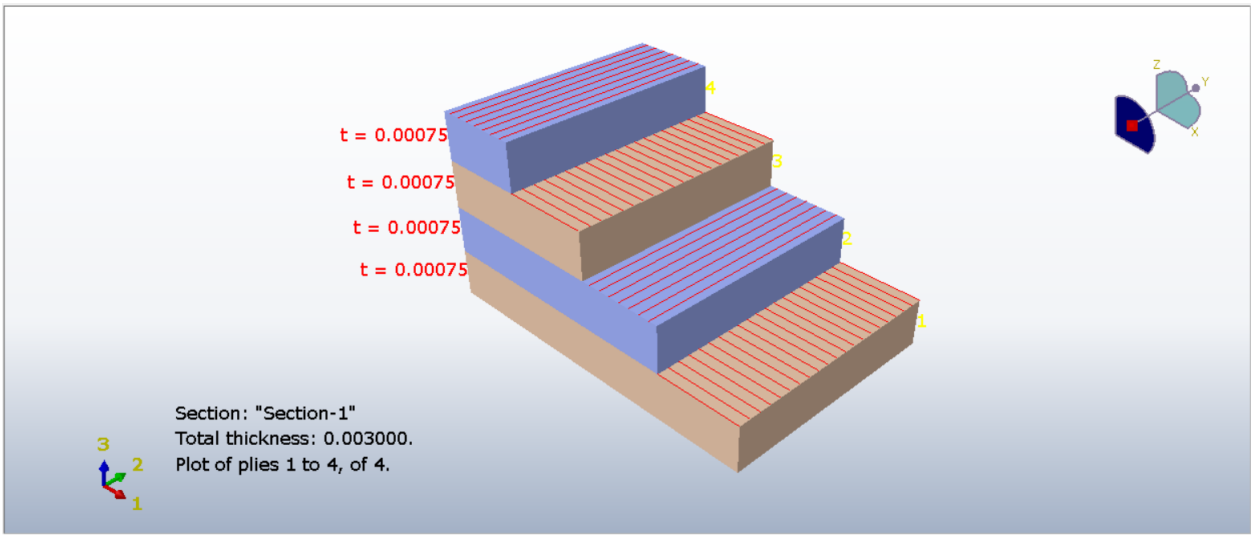

Figure 11. Composite lay-up stacking sequence for symmetry model of ENF.

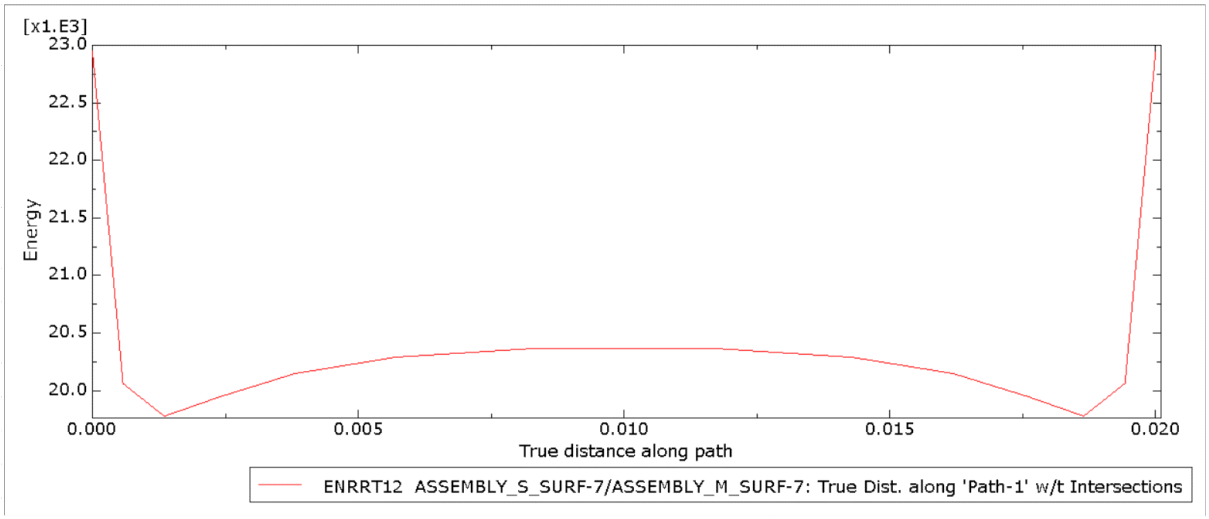

Figure 12. the energy release rate at the crack front using VCCT method ($ENRRT_{12}$) for ENF simulation.

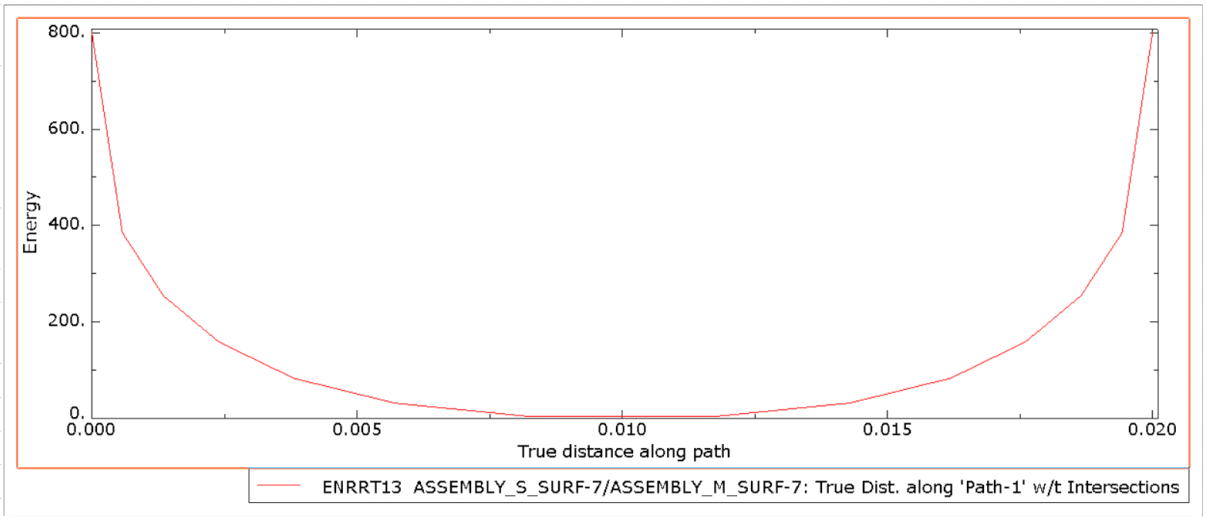

Figure 13. the energy release rate at the crack front using VCCT method ($ENRRT_{13}$) ENF simulation.

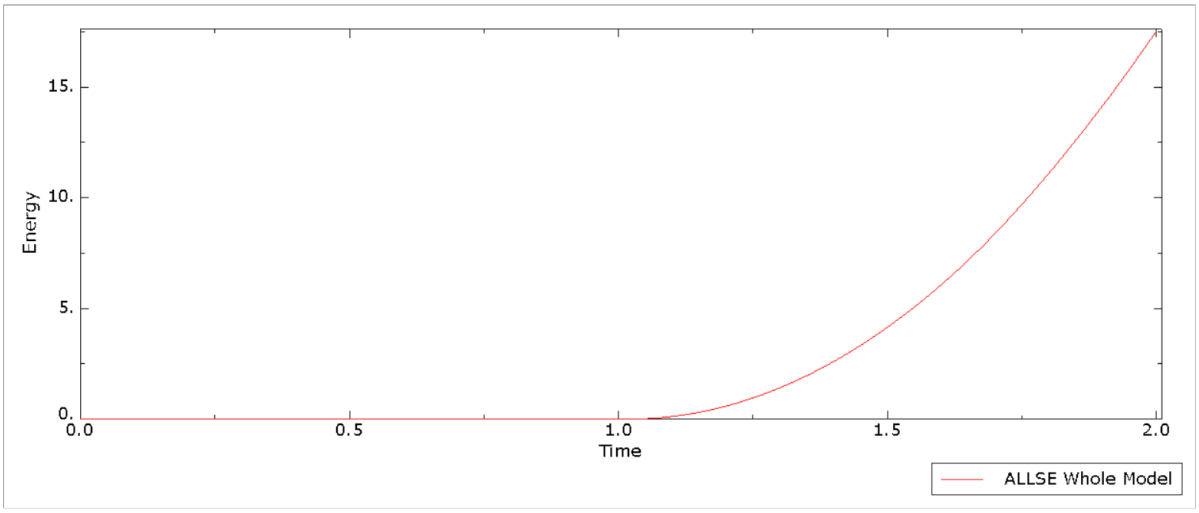

Figure 14. Strain-energy release rate versus time graph Abaqus result for the ENF model.